

Aging affects the phase coherence between spontaneous oscillations in brain oxygenation and neural activity*

Juliane Bjerkan^a, Gemma Lancaster^a, Bernard Meglič^b, Jan Kobal^b, Trevor J. Crawford^c, Peter V. E. McClintock^a, Aneta Stefanovska^{a,*}

^aLancaster University Department of Physics, LA1 4YB, Lancaster, United Kingdom

^bUniversity of Ljubljana Medical Centre Department of Neurology, 1525, Ljubljana, Slovenia

^cLancaster University Department of Psychology, LA1 4YF, Lancaster, United Kingdom

Abstract

The risk of neurodegenerative disorders increases with age, due to reduced vascular nutrition and impaired neural function. However, the interactions between cardiovascular dynamics and neural activity, and how these interactions evolve in healthy aging, are not well understood. Here, the interactions are studied by assessment of the phase coherence between spontaneous oscillations in cerebral oxygenation measured by fNIRS, the electrical activity of the brain measured by EEG, and cardiovascular functions extracted from ECG and respiration effort, all simultaneously recorded. Signals measured at rest in 21 younger participants (31.1 ± 6.9 years) and 24 older participants (64.9 ± 6.9 years) were analysed by wavelet transform, wavelet phase coherence and ridge extraction for frequencies between 0.007 and 4 Hz. Coherence between the neural and oxygenation oscillations at ~ 0.1 Hz is significantly reduced in the older adults in 46/176 fNIRS-EEG probe combinations. This reduction in coherence cannot be accounted for in terms of reduced power, thus indicating that neurovascular interactions change with age. The approach presented promises a noninvasive means of evaluating the efficiency of the neurovascular unit in aging and disease.

Keywords: Neurovascular unit, aging, neurovascular dynamics, EEG, fNIRS, wavelet analysis

1. Introduction

A healthy brain requires sufficient supplies of glucose and oxygen to function properly, and any impairment of the vasculature will affect their delivery to the target cells. The brain and cardiovascular system work closely together in a common endeavour to match energy supply to demand. Their intimate relationship is reflected in the concept of the neurovascular unit (NVU) (35), corresponding to consideration of the neurons, astrocytes, microglia, pericytes, endothelial cells and basement membrane as a single functioning entity. In the process of aging, the brain undergoes structural (16; 24) and functional changes, and so also does the cardiovascular system. Knowledge of healthy aging can aid understanding of the mechanisms of pathological aging, as age is the biggest risk factor in the etiology of neurodegenerative diseases, such as Alzheimer's disease which appears to include accelerated aging of the brain (28).

The neurophysiological changes in the aging brain have been well documented through measures of its electrical and magnetic activities using electroencephalogram

(EEG) and magnetoencephalogram (MEG) recordings, respectively (31; 2; 34; 4; 22; 109; 88). Both the power of brain waves, and the functional connectivity patterns in the brain, have been shown to change with age.

The cardiovascular system is a closed system of vessels, where blood circulates, cyclically pumped by the heart and oxygenated by the lungs. It is well known that heart rate variability (1) decreases with aging, whereas the blood pressure (78; 76) increases. This has been linked to altered cognition in healthy people below 70 years old (107), thereby indicating the importance of a well-functioning cardiovascular system for brain health. More local to the brain, changes in cerebral blood oxygenation can be measured non-invasively using functional Near-Infrared Spectroscopy (fNIRS). Several investigations have found differences in oxygenation dynamics between younger and older subjects, both in the resting state and during task activation (114). In elderly subjects, the power and connectivity in the 0.052–0.145 Hz range are reduced compared to younger ones (57; 110). This frequency range is associated with vasomotion, the mechanism through which smooth muscle cells modulate the blood flow, by altering the diameter of the blood vessels (40; 85; 97). However, despite general awareness that all components of the NVU are individually affected by aging (56), no quantitative method is available for non-invasive assessment of the function of the NVU as a whole. Nor has any study to date inves-

*Work supported by the Engineering and Physical Sciences Research Council (UK), the Sir John Fisher Foundation, and the Slovene Research Agency.

*Corresponding author

	N	Age (yrs)	Sex	BMI (kg m^{-2})	sBP (mmHg)	dBp (mmHg)
Younger	21	31.1 ± 6.9	11F/10M	23.6 ± 3.6	122 ± 18	79 ± 9.8
Older	24	64.9 ± 6.9	15F/9M	26.9 ± 3.0	136 ± 17	83 ± 11
p	-	1.02×10^{-8}	-	0.002	0.004	0.067

Table 1: Participants’ data. Age, body mass index (BMI), systolic blood pressure (sBP) and diastolic blood pressure (dBp) are given as means \pm standard deviations. p is obtained from the Wilcoxon rank-sum test between the two groups.

49 tigated directly whether changes with aging occur in the
50 interactions between the dynamics of blood oxygenation
51 and neural activity.

52 The purpose of the present study is to evaluate the ef-
53 ficiency of interaction between the vascular and neural
54 systems within the brain. We aim to investigate, on a
55 macroscopic scale, the dynamics of oxygen supply and the
56 dynamics of the neurons including the signalling of their
57 needs. We do so by determination of the coherence be-
58 tween spontaneous oscillations in blood oxygenation (mea-
59 sured using fNIRS) and electrical activity (measured si-
60 multaneously using EEG). Their coherence quantifies their
61 strength of interaction, which can be taken as a proxy for
62 the efficiency of the NVU. We hypothesise that it will be
63 altered in the aging population due to the structural and
64 functional changes in the brain. Because resting-state net-
65 works spanning several brain regions have been observed in
66 both EEG and fNIRS studies (114; 62; 18), and because
67 fNIRS and EEG have previously been found to exhibit
68 long range correlations (70), we determine the coherence
69 between all signal pairs. As the cerebrovascular system
70 depends on the systemic support of the cardio-respiratory
71 system, we also recorded heart rate and respiration. This
72 allows us to consider the physiological origin of the much-
73 discussed ~ 0.1 Hz oscillations (71; 108; 70; 111; 81; 72).

74 To follow the non-linear and time-variable dynamics
75 over many time-scales and to allow for resolution in both
76 time and frequency, we have employed wavelet phase co-
77 herence (WPC) (5) and a novel method of tracing the in-
78 stantaneous phases of oscillations by ridge extraction (39).
79 WPC is more resilient against artifacts than amplitude-
80 based coherence measures and, in addition, provides for
81 logarithmic frequency resolution. Given that frequency
82 and time are inversely related, this makes the method
83 more suitable than those with linear resolution, such as
84 the Fourier transform, and is particularly advantageous
85 when studying low frequency oscillations.

86 By comparing the analyses of measurements on groups
87 of younger and older participants in the resting state, we
88 seek evidence for changes in the phase interactions between
89 their neural and cardiovascular systems, and thus for age-
90 related changes in the efficiency and health of the NVU.

2. Methods

2.1. Participants

93 All participants provided written informed consent, and
94 the study was conducted in accordance with the Declara-
95 tion of Helsinki. The study protocols were approved by
96 the Commission of the Republic of Slovenia for Medical
97 Ethics and/or by the Faculty of Science and Technology
98 Research Ethics Committee (FSTREC) at Lancaster Uni-
99 versity. The study involved the recording and analysis of
100 data from 45 participants. The younger group consisted of
101 21 participants between 20 and 39 years. The older group
102 consisted of 24 participants between 56 and 77 years. Par-
103 ticipant details are provided in Table 1. The exclusion
104 criteria were neurodegenerative disorders, clinically diag-
105 nosed neurological disorders, psychiatric disease and/or di-
106 abetes. **Three participants were excluded because they fell**
107 **asleep during the measurements, and one participant was**
108 **excluded on account of poor probe contact resulting in**
109 **noisy data.**

110 Based on two groups with 21 and 24 participants, a sta-
111 tistical power of 0.8 and a significance level of 0.05 we
112 expected, at minimum, to reliably detect effects of size
113 0.92, which were considered large effects (23). Effect size
114 was calculated using Cohen’s d (15). Further details are
115 reported in the Supplementary Material (SM) Sec. 2.

2.2. Data acquisition

116 Data were recorded in quiet rooms at the Neurologi-
117 cal Clinic, Ljubljana, Slovenia or in the Nonlinear and
118 Biomedical Physics Lab, Physics Department, Lancaster
119 University, Lancaster, UK (see SM, Sec. 5). The same
120 system was used in both locations. Each participant was
121 seated in a comfortable chair and had their eyes open dur-
122 ing the approximately 30 minutes of measurement. No fix-
123 ation points were used. An electroencephalogram (EEG)
124 was recorded at 1 kHz using a 16-channel system (V-
125 Amp, Brain Products, Germany). Simultaneously, func-
126 tional Near-Infrared Spectroscopy (fNIRS) measurements
127 detected changes in oxygenated hemoglobin. **Note that**
128 **we refer to these measurements as “brain oxygenation”**
129 **although, strictly speaking, we investigate brain oxygena-**
130 **tion dynamics, because fNIRS does not measure absolute**
131 **hemoglobin concentrations.** An 8-source/8-detector LED
132 system (NIRScout, NIRx, Germany) was used and the
133

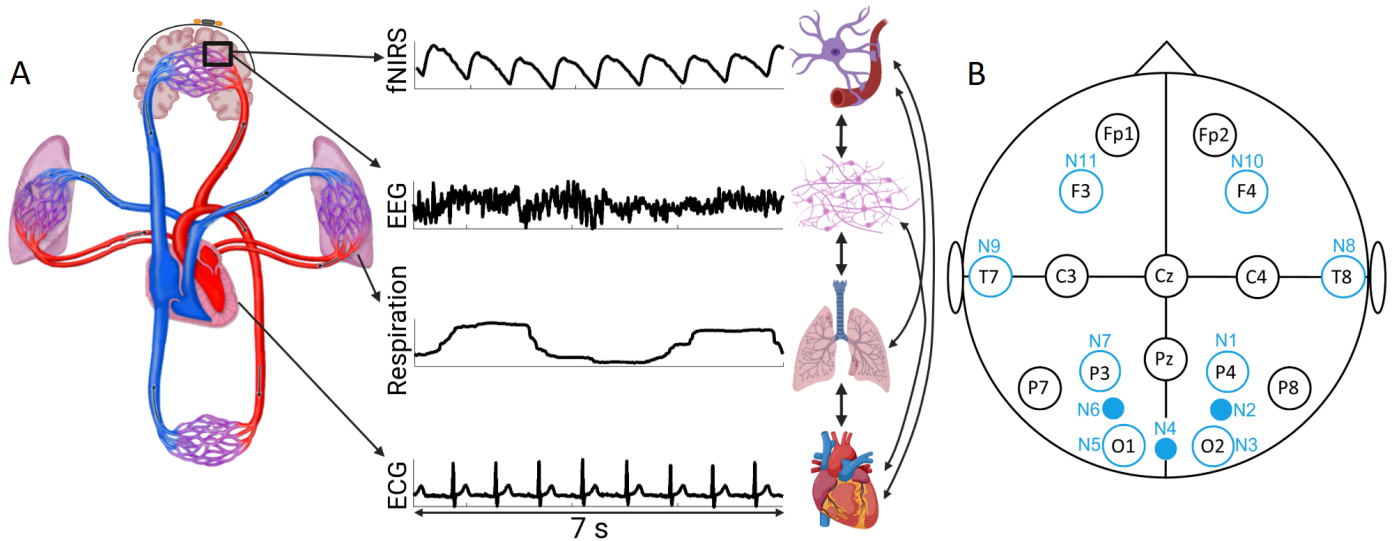


Figure 1: A) The cardiovascular system and brain, illustrated schematically with a zoom to show the neurovascular unit (NVU), and examples of recorded signals: fNIRS to capture brain oxygenation, EEG to capture the electrical activity of the brain, and respiration and ECG to capture systemic effect of the blood circulation. The vertical arrows show the combinations for the phase coherences investigated. B) Sketch illustrating the 16 EEG electrode (black) and 11 fNIRS probe (light blue) placements. Note that 8 EEG and fNIRS probes (indicated with blue open circles) are co-located.

recordings were made at 31.25 Hz. The probe layout is shown in Fig. 1B.

The heart rate was evaluated from an electrocardiogram (ECG), obtained with a bipolar precordial lead similar to the standard D2 lead. To maximize R-peak sharpness, electrodes were positioned on the right and left shoulders and over the lower left rib. The respiration rate was evaluated from the respiratory effort recorded using a belt wrapped around the participant’s chest, fitted with a Biopac TSD201 Respiratory Effort Transducer (Biopac Systems Inc., CA, USA). Both were sampled at 1.2 kHz using a signal conditioning system (Cardiosignals, Institute Jožef Stefan, Slovenia). Fig. 1A depicts signals from a participant in the younger group.

2.3. Data preparation and preprocessing

Signal processing was done in MATLAB, and the analysis was completed using the toolbox MODA (69) to implement the methods illustrated by Clemson et al. (13). A continuous 25-minute signal, mostly free of movement artifacts, was extracted for each participant. The data were detrended by subtracting a best-fit third-order polynomial, and bandpass filtered in the range 0.007–4 Hz. The preprocessing procedures were as described by Iatsenko et al. (37). To reduce computational load, the EEG, ECG and respiration signals were each downsampled using a moving average. The resultant frequencies are listed in Table 2. The artefact in the EEG signals due to cross-talk between brain electrical activity and the electrical activity of the heart was extracted using nonlinear mode decomposition (38).

As we do not have individual 3D head geometry data, such as MRI scans, and as we use a relatively low-density

EEG set-up, we chose to do the analysis on the sensor level rather than the source level. This is because a lack of geometrical data coupled with a low-density of EEG sensors is known to result in a low accuracy of source localisation (9; 63). Increasing the number of electrodes would have improved spatial localisation to some extent, but would also have increased the set-up time for the experiment, constituting a limiting factor in clinical applications.

2.4. Time-frequency analysis

Time-frequency analysis provides information on how the frequency of an oscillation changes through time. We used the continuous wavelet transform (WT) and, at each discrete time t_n and frequency ω_k , obtained a complex number $X_{k,n} = a_{k,n} + ib_{k,n}$. From this a phase Φ and amplitude A were found:

$$\Phi_{k,n} = \arctan \left(\frac{b_{k,n}}{a_{k,n}} \right),$$

$$A_{k,n} = |X_{k,n}|.$$

Power was found by squaring the amplitude. The WT has a logarithmic frequency scale. When analysing low frequency oscillations, the WT therefore provides better frequency resolution than, for example, the windowed Fourier transform. After taking the transforms, the time-averaged WT power spectra were calculated for each of the 11 fNIRS signals, and for the instantaneous heart/respiration rates. The Morlet wavelet was used for the WT. An overview of the parameters used, including the frequency resolution and sampling frequencies, is provided in Table 2.

Analysis	Method	Parameters
Heart rate	Peak detection and ridge extraction	WT: $f_0 = 2$ $f \in [0.6, 1.7]$ $f_s = 100$ Hz
Respiration rate	Peak detection and ridge extraction	WT: $f_0 = 1$ $f \in [0.1, 0.6]$ $f_s = 100$ Hz
γ instantaneous frequency	Ridge extraction	WT: $f_0 = 5$ $f \in [20, 30]$ $f_s = 142$ Hz
γ instantaneous power	WT and frequency average	WT: $f_0 = 5$ $f \in [20, 30]$ $f_s = 142$ Hz
IHR/IRR power	Time-averaged WT	WT: $f_0 = 1$ $f \in [0.007, 2]$ $f_s = 20$ Hz
EEG wavelet power	Time-averaged WT	WT: $f_0 = 1$ $f \in [0.007, 4]$ $f_s = 31.25$ Hz
fNIRS wavelet power	Time-averaged WT	WT: $f_0 = 1$ $f \in [0.007, 4]$ $f_s = 31.25$ Hz
Power of γ instantaneous frequency/power	Time-averaged WT	WT: $f_0 = 1$ $f \in [0.007, 4]$ $f_s = 142$ Hz
fNIRS-EEG coherence	Wavelet phase coherence	WT: $f_0 = 1$ $f \in [0.007, 4]$ $f_s = 31.25$ Hz
fNIRS-fNIRS coherence	Wavelet phase coherence	WT: $f_0 = 1$ $f \in [0.007, 4]$ $f_s = 31.25$ Hz
EEG-EEG coherence	Wavelet phase coherence	WT: $f_0 = 1$ $f \in [0.007, 4]$ $f_s = 20$ Hz WFT: $f \in [4, 48]$ $f_s = 142$ Hz
IHR/IRR/Respiration fNIRS/EEG coherence	Wavelet phase coherence	WT: $f_0 = 1$ $f \in [0.007, 2]$ $f_s = 20$ Hz
γ IF-fNIRS/ γ IP-fNIRS coherence	Wavelet phase coherence	WT: $f_0 = 1$ $f \in [0.007, 4]$ $f_s = 31.25$ Hz

Table 2: Summary of the methods and parameters used in the analyses. IHR and IRR – instantaneous heart and respiratory rates (frequencies) respectively; γ IF – instantaneous frequency of oscillations in gamma band; γ IP – instantaneous power of oscillations in gamma band; WT – wavelet transform; WFT – windowed Fourier transform; f_0 – frequency resolution f_s – sampling frequency.

2.5. Wavelet phase coherence

Wavelet phase coherence (WPC), introduced by Bandrivskyy et al. (5), is used to evaluate how consistent the phase difference between two oscillations remains over time. The phase coherence is evaluated at each frequency, and the values of coherence and phase difference are originally evaluated at each time.

The WPC does not assume stationarity of the time-series and is particularly suitable when the non-

stationarity comes from a time-variation of the characteristic frequencies. The logarithmic frequency resolution of WPC is particularly suitable for signals with a large span of characteristic frequencies. It provides a model-free approach that does not assume the existence of an underlying stochastic process. Taken together with wavelet analysis, it provides information about potential oscillatory modes contributing to the measured signal, and their degree of coordination and interaction. However, it does not provide information about direction of interaction, nor about couplings between oscillatory modes. For the evaluation of directional couplings one may use dynamical Bayesian inference, Granger causality, or similar information- or permutation-based methods (13; 95; 96).

The phase coherence is evaluated at each frequency and takes a value between 0 and 1. If the phase difference remained constant throughout the whole length of the signals at a certain frequency, the phase coherence value would be 1 at that frequency. As the measure only depends on the phase difference, it is independent of the amplitudes of the oscillations. The phase difference between signals 1 and 2 at time t_n and frequency ω_k is

$$\Delta\Phi_{k,n} = \Phi_{k,n}^{(2)} - \Phi_{k,n}^{(1)}.$$

The wavelet phase coherence is then defined as

$$C_{\Phi}(\omega_k) = \sqrt{\langle \cos \Delta\Phi_{k,n} \rangle^2 + \langle \sin \Delta\Phi_{k,n} \rangle^2},$$

where $\langle \cos \Delta\Phi_{k,n} \rangle$ and $\langle \sin \Delta\Phi_{k,n} \rangle$ are averaged in time.

We assessed the fNIRS–fNIRS pairwise coherence (for all permutations of the 11 fNIRS probes), as well as the EEG–fNIRS, instantaneous heart rate (IHR)–respiration, IHR–EEG, IHR–fNIRS, respiration–fNIRS, respiration–EEG, instantaneous respiration rate (IRR)–fNIRS, and IRR–EEG coherences.

2.6. Frequency bands

The sampling frequency of the fNIRS is 31.25 Hz, and so the Nyquist frequency would be ~ 15 Hz. If the oscillations had constant frequencies, and there were no harmonics, then 15 Hz would have been the upper limit for investigation of oscillatory modes and their interactions in the fNIRS signal. Furthermore, fNIRS is known not to contain oscillations faster than the cardiac oscillation (~ 1 Hz). Consistent with this, we did not see any significant power above the cardiac frequency. So, we selected the upper frequency limit to be 4 Hz for the fNIRS and fNIRS-EEG interactions. The EEG signal was sampled at 1000 Hz, but we analysed it only up to 48 Hz, which allowed for investigation of the slow γ oscillatory modes. The other reason for our 48 Hz limit was to avoid the effect of the 50 Hz notch filter used by the monitoring system. For both the EEG and fNIRS, the lower frequency limit was set to 0.007 Hz.

The power and coherence values were divided into the conventional frequency bands (Table 3) (97), within each

of which an average value was calculated. The first five bands, representing the characteristic frequency intervals of the cardiovascular system (97), strongly overlap the slow oscillations in EEG (11). The last five bands are the traditional EEG frequency bands. After obtaining single power/coherence values in each band for each subject, the two groups were compared.

Name	Frequency range (Hz)
Endothelial (V)	0.007 – 0.021
Neurogenic (IV)	0.021 – 0.052
Myogenic (III)	0.052 – 0.145
Respiratory (II)	0.145 – 0.6
Cardiac (I)	0.6 – 1.7
Delta (δ)	1.7 – 4
Theta (θ)	4 – 7.5
Alpha (α)	7.5 – 14
Beta (β)	14 – 22
Gamma (γ)	22 – 48

Table 3: Frequency ranges used in the analysis (97). The cardiac and δ ranges are slightly changed from past studies (see text).

In previous studies of cardiovascular dynamics, the cardiac band was defined as 0.6–2 Hz (97). In the present case, however, we also need to take account of EEG dynamics which potentially overlap the cardiac band. To separate the cardiac and δ bands, we therefore defined the cardiac band as 0.6–1.7 Hz and the δ band as 1.7–4 Hz. With the upper limit set to 1.7 Hz, the variation in heart rate is still accommodated.

The respiratory oscillations are manifested in the frequency interval 0.145–0.6 Hz. They can be detected even in the smaller vessels such as capillaries, as they generate pressure waves that propagate throughout the entire cardiovascular system (99).

The 0.052–0.145 Hz frequency interval is referred to as myogenic, and the neurogenic band is defined as 0.021–0.052 Hz. The origins of these two bands are still debated, with perceptions depending on whether interest is being focused on the vascular or cardiac regulation mechanisms (see discussion section). The neurogenic response is similar to the myogenic response in that it also depends on pressure changes, but additionally involves neuronal pathways.

The frequency intervals 0.005–0.021 Hz is called the NO-dependent endothelial frequency band, in view of evidence that NO-dependent endothelial activity manifests itself within this range (50; 97; 91).

2.7. Heart and respiration rates

Time-series of instantaneous heart and respiration rates were obtained in two ways: by peak detection and by the ridge extraction method. Peak detection was performed in the time domain with a customised program in MATLAB that searched for R-peaks in the ECG signals or maxima in the respiration signal. The instantaneous frequencies were

extracted in the time-frequency domain by the ridge extraction method (39) using the toolbox MODA (69). Note that “instantaneous heart rate” (IHR) is a time-series of heart frequency values. It is traditionally referred to as heart rate variability when derived in the time domain from the intervals between heart beats. Similarly, “instantaneous respiration rate” (IRR) is a time-series of respiration frequency values, and is usually called respiration rate variability when derived from the time intervals between maxima. The instantaneous heart and respiration rate time series were in close agreement whether obtained either by the peak detection method or by the ridge extraction method, as shown in Fig. 2 for the IHR. The average heart and respiration rates were obtained from their respective time-series.

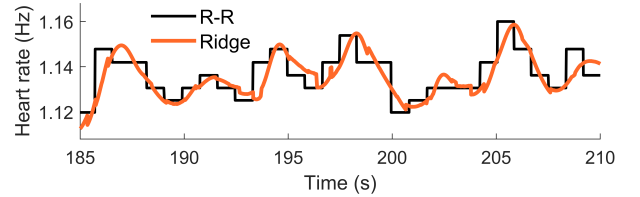


Figure 2: Comparison of the IHR found by R-R peak detection with that found by ridge extraction. We use the lognormal wavelet (37) with a frequency resolution of 2Hz. It has a better trade-off between time and frequency resolution than the Morlet wavelet.

Because the time-series obtained with the ridge extraction method are smooth functions, ready to use in time-series analysis, they were used in the wavelet and phase coherence analyses. Furthermore, the ridge extraction method is more appropriate for extracting IHR than the peak-detection method, as ridge extraction takes into account the whole ECG signal and not just the R-peaks, thus also capturing the effect of T-waves.

For the IHR, ridge extraction was applied to the WTs of ECG signals in the 0.6–1.7 Hz frequency range. The lognormal wavelet and a frequency resolution of 2 Hz were used for the WT. The sampling frequency of the IHR was the same as that of the ECG, and no interpolation was needed (36). For the IRR, ridge extraction was applied to the WTs of respiration signals in the 0.1–0.6 Hz frequency range and with a frequency resolution of 1 Hz.

The standard deviation of the instantaneous rates (sd IHR and sd IRR), resulting in a single number in each case, was used to obtain a measure of their variability.

2.8. Frequency and amplitude modulation of the γ -band by low-frequency oscillations

From the EEG signals, the instantaneous frequency and power in the 20–30 Hz interval were obtained by ridge extraction (39), and are referred to as a γ -instantaneous frequency and γ -instantaneous power time-series. Fig. 3 illustrates the procedure. The frequency resolution parameter was 5 Hz.

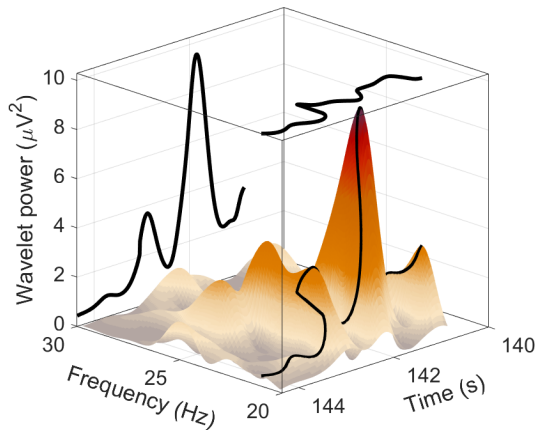


Figure 3: γ -instantaneous frequency (projected onto the Frequency-Time plane) and γ -instantaneous power time-series (projected onto the Wavelet power-Time plane) as obtained by ridge extraction.

For the 8 locations where fNIRS and EEG sensors are co-located, the WPC was calculated between the γ -instantaneous frequency time-series and the fNIRS signal, to evaluate the effect of low frequency modulation on the oscillations in the γ -band. The WPC was also calculated between the γ -instantaneous power time-series and the fNIRS signal to evaluate the effect of low frequency modulation on the γ -band amplitude and the corresponding power.

2.9. Intersubject surrogates

To ensure that apparent coherence is statistically significant, we used intersubject surrogates (52). In addition to calculating coherence between the signals from one person, we calculated the apparent coherence between signals from different participants. This measure of coherence could not signify any underlying link between the signals, and was thus random. Inter-subject surrogates have previously been found suitable in the context of cardiorespiratory interactions (36). They are model-free and do not require stationary data.

Based on 154 intersubject surrogates a surrogate threshold was set as the 95th percentile of all these coherences at each frequency. In the plots throughout the paper, only the effective coherence (i.e. coherence after subtracting the surrogate threshold) is shown, and it was the effective coherence that we used in testing for differences between the groups. Each subject and signal pair had an individual significance threshold to account for different spectral biases in the signals. Due to the lower number of complete oscillations at low frequencies, the likelihood of apparent coherence is increased. Hence, the surrogate threshold is high for low frequencies and, correspondingly, the measurement time is not long enough for a reliable study of oscillations in the endothelial band in the case of fNIRS-EEG coherence.

2.10. Group statistics

To assess population differences, the non-parametric two-sided Wilcoxon rank-sum test was applied, and differences are considered significant for $p < 0.05$. The data are presented as median values and violin plots (33). Additionally, for the fNIRS, EEG and fNIRS-EEG analyses, a Monte-Carlo permutation test (58) was applied to check the reliability of the significance. From the total of 45 participants, 21 were randomly placed in one group and 24 in the other. The Wilcoxon rank-sum test was applied to test for differences between the permuted groups. After 16587 permutations the original p -value was compared with the values obtained with permutation. If the initial p -value was smaller than 95% of the p -values obtained by permutations its significance was considered confirmed. Additional details are provided in Sec. 7 of the SM.

In time-frequency analysis, cluster-based permutation is a common method to correct for multiple comparisons (58). As we averaged in both time and frequency before applying statistical tests, we would only see differences in power/coherence that were present over many time-points and frequencies. For the spatial aspect of multiple comparisons, the expected false discovery rate, quantifying how many null-hypotheses would be incorrectly rejected with $\alpha = 0.05$ assuming all null-hypotheses were true, was 0.8 for the EEG power analysis, 0.55 for the fNIRS power analysis, 6 for the EEG coherence analysis, 2.75 for the fNIRS coherence analysis and 8.8 for the fNIRS-EEG coherence analysis. From N trials, and assuming that there were no true differences, the probability of obtaining X or more positive findings was calculated from the binomial probability. This was used to assess the reliability of the results, keeping the multiple comparison problem in mind, as done in the literature (66; 70).

2.11. Correlations

The correlations were found from the Spearman's rank-order correlation, which is a non-parametric alternative to the Pearson linear correlation. It tests for a monotonic relationship between two variables. The p -value was found from permutation distributions.

3. Results

Here we present the results of the analyses summarised in Table 2. These include the *central* oscillations of the cardiovascular system (evaluated from the instantaneous heart and respiration frequencies), and the *local* vascular and neural oscillations in the brain (from fNIRS and EEG). The analyses relate to the transport of nutrients to the NVU, quantifying its efficiency and the impact of ageing.

3.1. Central oscillations: heart and respiration rates

We first present the cardio-respiratory characteristics. This enables a consistency check with earlier results, and

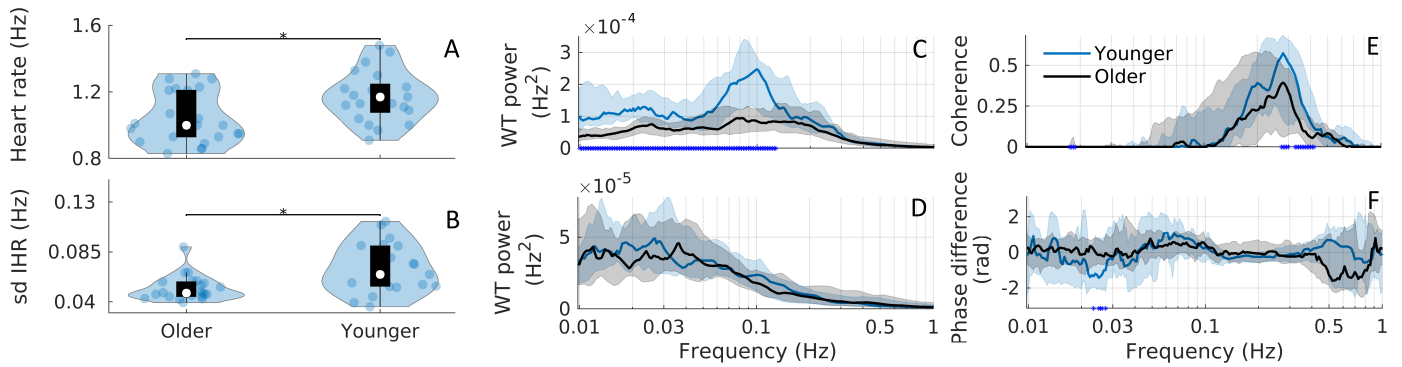


Figure 4: Violin plots for A) heart rate, and B) its variability as quantified by the standard deviation (sd) of the IHR for the older and younger groups. The black stars indicate significant differences, $p < 0.05$, between groups. The white circles indicate the group medians. C) Time-averaged wavelet transform power of the IHR. D) Time-averaged wavelet transform power of the IRR. E) IHR–respiration coherence. F) Average phase differences between IHR and respiration, given in radians. A negative phase difference indicates that respiration is the leading signal. The blue and black lines are the median group power/coherence/phase difference, while the shaded areas show the 25–75th percentiles. Significant differences ($p < 0.05$) between the groups at particular frequencies are indicated by blue stars on the x -axis (causing effective thickenings of the axis).

provides insight into systemic changes relevant to neurovascular interactions,

Heart rates (older: 1.04 ± 0.16 Hz; younger: 1.17 ± 0.15 Hz) and sd IHR (older: 0.052 ± 0.011 Hz; younger: 0.070 ± 0.022 Hz) are significantly different between the groups ($p = 0.014$, $p = 0.005$), as shown in Fig. 4A,B. No significant difference is seen in the respiration rate (older: 0.23 ± 0.08 Hz; younger: 0.24 ± 0.05 Hz, $p = 0.300$), or sd IRR (older: 0.039 ± 0.009 Hz; younger: 0.045 ± 0.019 Hz, $p = 0.26$). The corresponding plots are shown in the SM Sec. 3.

IHR power is reduced in the older group in the 0.01–0.11 Hz range (see Fig. 4C). The IRR power is not significantly different between the groups (Fig. 4D).

Each group has significant IHR–respiration coherence in the respiratory band (see Fig. 4E; for the frequency band ranges, see Table 3). The younger group has significantly higher coherence around 0.3 Hz, compared to the older group. For both groups the IHR power and IHR–respiration coherence were shown not to differ significantly between males and females (see SM Sec. 6), consistent with earlier results (36).

3.2. Interactions between instantaneous heart/respiration rates and brain oxygenation

The results presented here illustrate how the modulation of the heart and respiration rates is linked to the oxygenation of the brain. Fig. 5 shows the wavelet phase coherence between IHR and oxygenation, between IRR and oxygenation, and between the respiration signal and oxygenation, all at N5. For data from the other fNIRS probes see SM Sec. 3. The SM also includes the IHR–EEG, respiration–EEG and IRR–EEG coherence.

There are systematic differences in coherence, with the older group tending to have lower coherence. This difference is statistically significant for coherence between

IHR and oxygenation (Fig. 5A), and is particularly pronounced in the myogenic and respiratory bands. The same significant reduction of coherence with age is observed in coherence between the IHR and all other oxygenation signals apart from the two temporal ones, where the coherence is reduced only in the respiratory band. Interestingly, the phase difference between oxygenation and IRR/respiration/IHR is found to be negative in the respiratory band, meaning that brain oxygenation is the leading signal. This result is consistent for both age groups. In contrast, the phase difference in the myogenic region is slightly positive, indicating that the brain oxygenation lags.

3.3. Brain oxygenation oscillations

Here we present the power calculated for all 11 fNIRS signals, and coherence between all possible signal combinations. The positions of the probes are shown in Fig. 1B.

The myogenic power (0.052–0.145 Hz frequency interval) in 8 of the 11 channels is significantly lower in the older group (Figs. 6A,B). A lower power is also found in the endothelial, neurogenic and respiratory bands (Fig. 6B), but the differences are statistically significant for fewer probes. In the endothelial band there are 3 fNIRS probes with a significant difference between the groups, while this number is 4 in the respiratory band, and 1 in the neurogenic and cardiac bands. The chance of obtaining 3 positive outcomes out of 11 is 1.5% when there were no true differences, while the chance of obtaining 1 positive outcome out of 11 is 43% when there were no true differences.

Significantly lower myogenic coherence in the older participants is found in 12 fNIRS signal combinations: across the frontal-parietal signals, the frontal signals and the occipital signals (Fig. 6C,D). In the neurogenic band significantly higher coherence in 12 fNIRS combinations (mainly from the temporal probes) is observed in the older group.

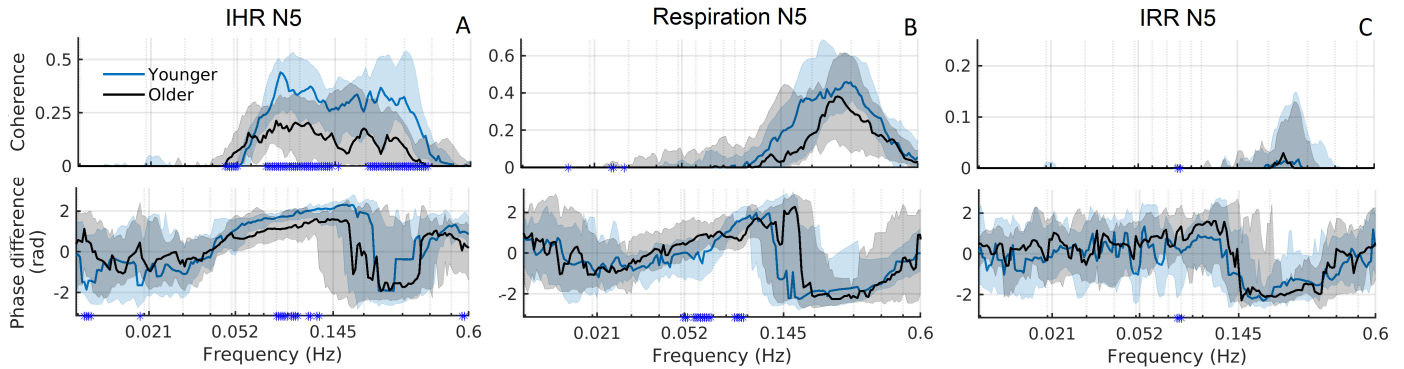


Figure 5: **Coherence (upper panels) and phase difference (lower panels)** between A) IHR and N5, B) respiration rate and N5, C) IRR and N5. Note that the y -axes differ. See Fig. 1 for the locations of the EEG electrodes and fNIRS probes. The blue and black lines represent the younger and older group medians, respectively, while the shaded areas show the 25–75th percentiles. Significant group differences at particular frequencies are indicated by blue stars on the x -axis. Phase differences are given in radians, and a negative value indicates that N5 is the leading signal.

In the cardiac band in 50 of 55 combinations coherence is also significantly higher in the older group. The differences are found between the frontal-parietal, frontal-occipital and temporal signals. In the endothelial band coherence in 3 combinations is significantly higher in the older group, while in the respiratory band coherence in only one combination is significantly higher in the younger group. The chance of obtaining 12 positive outcomes out of 55 is 0.0014% when there were no true differences, while the chance of obtaining 3 positive outcomes out of 55 is 52%.

Brain oxygenation for males and females is summarised in Sec. 6 of the SM. The older male group has higher myogenic power at probes 1 and 9 compared to the older female group, while the older female group has higher myogenic coherence than the older male group in 7 signal combinations.

3.4. Brain neuronal activity evaluated by EEG

The EEG power and coherence are consistent with previous results (61; 109; 88; 65; 83), and are summarised in the SM Sec. 4.

3.5. Coherence between neuronal activity and brain oxygenation

The coherence between neuronal activity, as evaluated by EEG, and brain oxygenation, as evaluated by fNIRS, differs significantly between the groups, in both the myogenic and cardiac bands (Fig. 7B,C). In the myogenic band, the coherence is lower in the older group in 46/176 probe combinations and the decrease does not seem confined to any specific areas. However, both groups have low myogenic coherence in the two temporal fNIRS probes (N8 and N9). In contrast, the coherence in the cardiac band is higher in the older group in 50/176 probe combinations. The chance of having 46 or more positive findings out of 176 is $1.2 \times 10^{-18}\%$ assuming there were no true differences. Further information is provided in the SM. It consists of

neurogenic and respiratory coherence (Fig. 23), the coherence plots of all 176 fNIRS-EEG combinations (Sec. 10), and the results divided by sex (Sec. 6).

3.6. Frequency and amplitude modulation of the γ -band by low-frequency oscillations

Here we show analysis of possible amplitude and phase modulation of γ -band oscillations by low-frequency oscillations. There is non-zero power for both the γ -instantaneous frequency and γ -instantaneous power time-series between 0.007 and 4 Hz (Figs. 8A, B) for both groups indicating the existence of modulation. The coherence between oxygenation and these time-series, and the phase shifts for both instances, are shown in Fig. 8C–F for the signals measured at location O1. For the remaining locations, see the SM Sec. 11. For the γ -instantaneous frequency time-series the coherence is zero for all frequencies in the interval 0.007–4 Hz. For the γ -instantaneous power time-series the median coherence is zero, but there is evidence of some significant effective coherence (Fig. 8D). For the oxygenation–power there is a negative phase shift for the older group around 0.06–0.08 Hz (Fig. 8F), which is significantly different between the groups in 5/8 probe combinations. A negative phase difference indicates that the oxygenation is lagging.

3.7. Correlations

BMI is negatively correlated with neurovascular coherence in the myogenic band, IHR–respiration coherence in the respiratory band and IHR–respiration coherence in the myogenic band (Fig. 9A,B,C). The systolic blood pressure is also negatively correlated with neurovascular coherence in the myogenic band ($\rho = -0.435$, $p = 0.004$) and IHR–respiration coherence in the respiratory band ($\rho = -0.356$, $p = 0.022$) (SM Sec. 8).

As shown in Fig. 10 the neurovascular coherence in the myogenic band is correlated with the IHR–respiration coherence in the myogenic band ($\rho = 0.397$, $p = 0.008$),

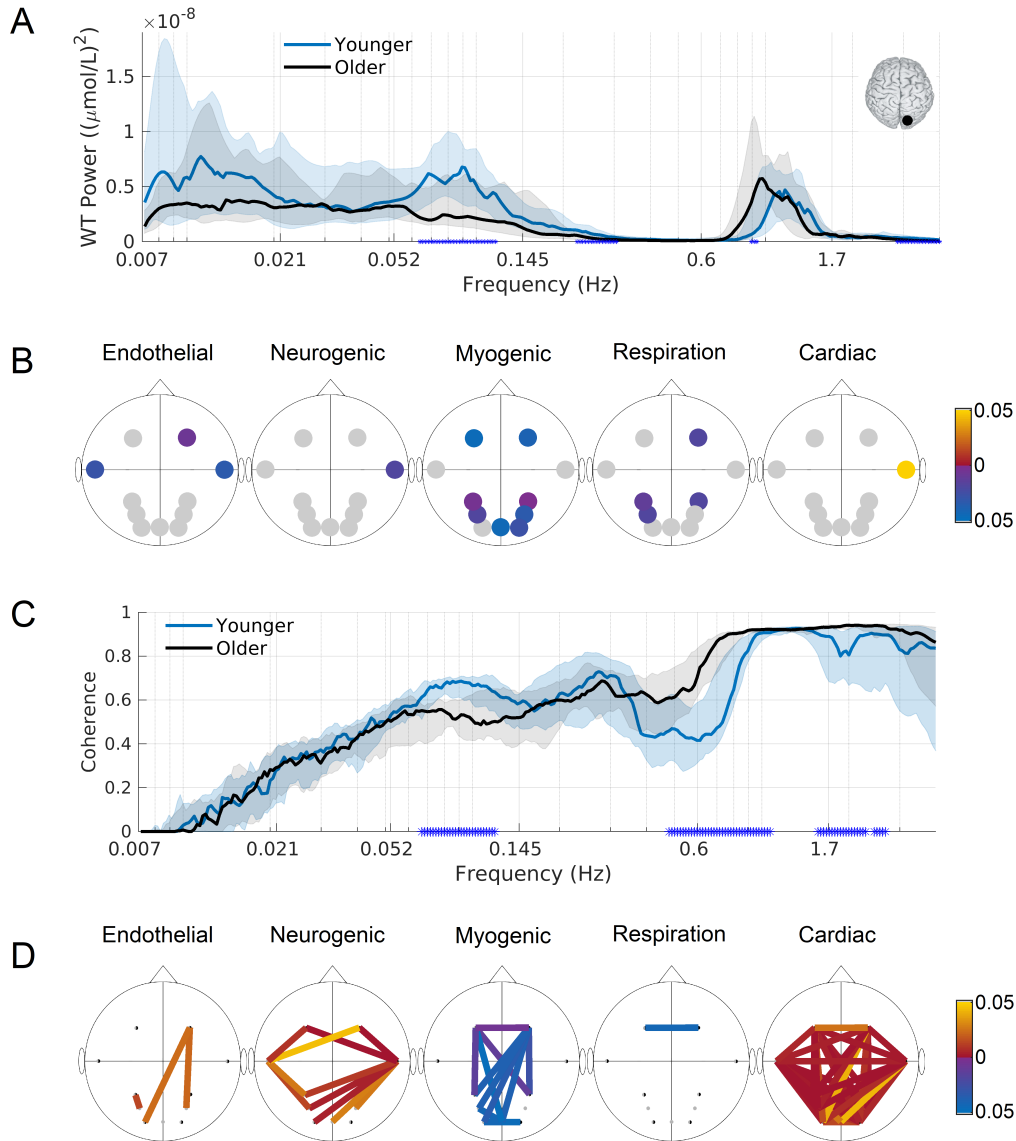


Figure 6: fNIRS power and coherence. A) Time-averaged power spectra for N3. B) p -values indicating significant group differences between the powers in the frequency bands. Blue (yellow) indicates that the power is higher in the younger (older) group. C) Coherence between N11 and N7 (see Fig. 1 for locations). The blue and black lines are the median group coherences, while the shaded areas show the 25–75th percentiles. Significant differences between the groups at particular frequencies are indicated by blue stars on the x -axis. D) p -values indicating a significant group difference between the coherence in the frequency bands. Blue (yellow) indicates that the coherence is higher in the younger (older) group. For the frequency intervals see Table 3, and for the probe lay-out see Fig. 1.

562 while this is not the case for the neurovascular coherence
 563 and the IHR–respiration coherence in the respiratory band
 564 ($\rho = 0.103$, $p = 0.504$).

565 4. Discussion

566 Based on 25-minutes signals recorded in participants in
 567 resting state and novel time-frequency analysis methods,
 568 our investigation of cardiovascular and neurovascular in-
 569 teractions reveals clear changes with aging. These are
 570 manifested through:

- 571 • Weakened 0.052–0.145 Hz coherence between the neu-
 572 ral activity and brain oxygenation, reflecting reduced

neurovascular interactions; 573

- 574 • Reduced coherence between instantaneous heart rate
 575 and brain oxygenation oscillations in the myogenic
 576 and respiratory frequency bands;
- 577 • Changes in the heart and respiration rates, and their
 578 coordination through respiratory sinus arrhythmia;
 579 and
- 580 • Altered brain oxygenation resting state networks in
 581 the brain.

We now discuss these changes in more detail. 582

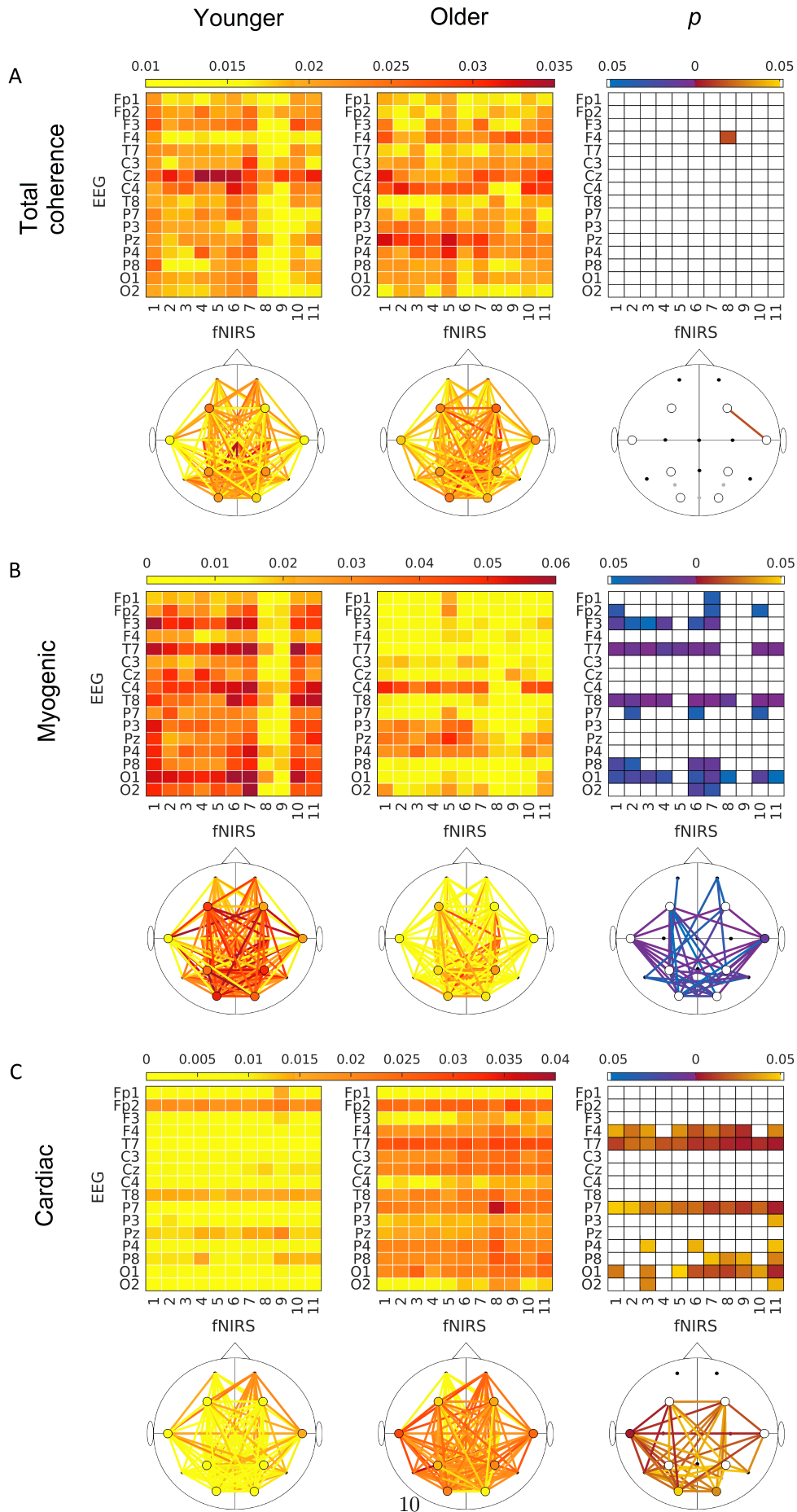


Figure 7: A) Group median fNIRS-EEG coherence averaged over the frequency band 0.021–1.7 Hz. The results for the younger group (left) are compared with those for older group (middle) and p -values indicating a significant difference between the groups are shown on the right. Blue (yellow) coding indicate that coherence is higher in the younger (older) group. B) Same as for A but for the myogenic band. C) Same as for A but for the cardiac band. For the frequency intervals see Table 3, and for the probe lay-out see Fig. 1.

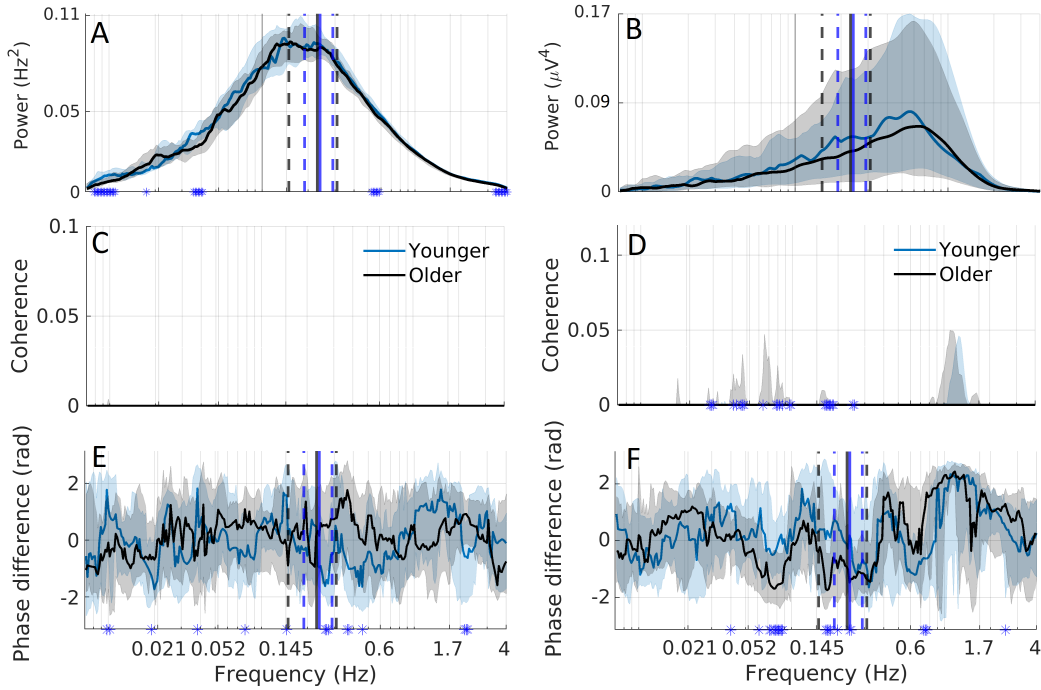


Figure 8: Comparisons between the older and younger groups related to frequency and amplitude modulation in the EEG γ -interval. Median power of the A) γ -instantaneous frequency time-series and B) γ -instantaneous power time-series. C) Median coherence between fNIRS and the γ -instantaneous frequency time-series. D) Median coherence between fNIRS and γ -instantaneous power time-series. E) Phase difference between fNIRS and the γ -instantaneous frequency time-series. F) Phase difference between fNIRS and the γ -instantaneous power time-series. The blue and black lines are the median group coherences, while the shaded areas show the 25–75th percentiles. Significant differences between the groups at particular frequencies are indicated by blue stars on the x -axis. The blue and black solid vertical lines indicate the average respiration rates for the younger and older group, while the red dashed lines indicate the standard deviations. Both fNIRS and EEG signals are from location O1.

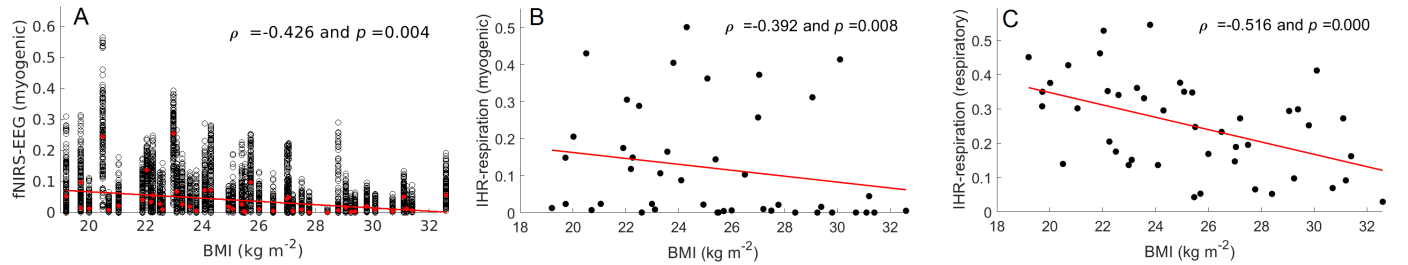


Figure 9: Spearman correlations between A) BMI and fNIRS–EEG coherence in the myogenic band, B) BMI and IHR–respiration coherence in the myogenic band, and C) BMI and IHR–respiration coherence in the respiratory band. In A) the black circles show the coherence values between fNIRS–EEG combinations (176 combinations per participant), while the red crosses show the median coherence for each participant. The correlation is found between the median coherence values and BMI.

4.1. Central oscillations: heart and respiration activity

Consistent with previous studies (36), we found a decrease in the variability of the cardiac frequency with age, as quantified by the sd IHR. Additionally, the average resting cardiac frequency (heart rate) is higher in the younger group. We did not find a significant reduction with age in the respiratory frequency band of the IHR (in studies with linear frequency resolution and shorter recordings often referred to as the high frequency band, 0.15–0.4 Hz, linked to parasympathetic nervous activity (1)). The IHR power decreases with age in the myogenic frequency band, 0.052–0.145 Hz. We note here that when evaluated with linear frequency resolution, and based on shorter, usually

5-min recordings, this frequency interval is also referred to as the low frequency band, 0.04–0.15 Hz, and is linked to sympathetic nervous activity (1)).

Note that the low/high frequency bands strongly overlap the myogenic/respiratory frequency bands. Low heart rate and insignificantly different respiratory band power in elderly participants could reflect relatively preserved parasympathetic tone. However, the changed parasympathetic/sympathetic activity is not sufficient to account for the variability in heart rate, which is generated by a complex interplay of nervous activity, respiration, smooth muscle cells and other factors (7; 14). Reduced variability with aging has previously been demonstrated (1; 27; 91),

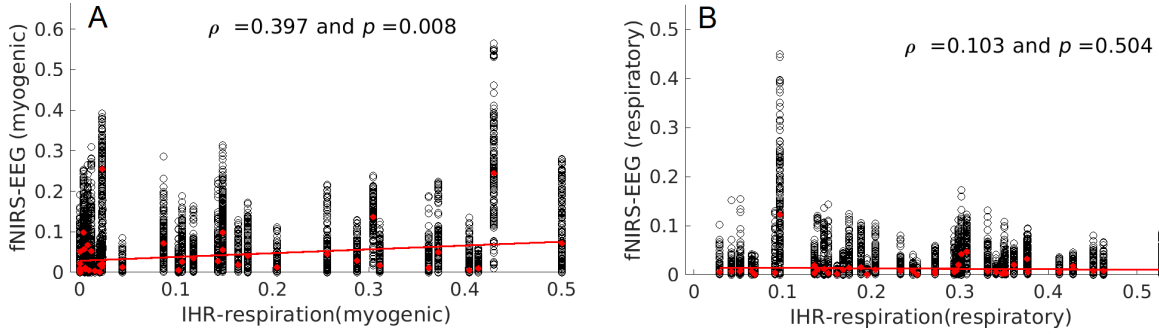


Figure 10: Spearman correlations between A) IHR–respiration coherence in the myogenic band and fNIRS–EEG coherence in the myogenic band, B) IHR–respiration coherence in the respiratory band and fNIRS–EEG coherence in the respiratory band. The black circles show the coherence values between fNIRS–EEG combinations (176 combinations per participant), while the red crosses show the median coherence for each participant. The correlation is found between the median coherence values and IHR–respiration coherence.

also with wavelet-based methods (36).

A tendency for the IHR–respiration coherence to be lower in the older group reaches significance at around 0.3Hz. We did not, however, find a significant change in the respiration rate or its variability, as evaluated by the sd IHR, so this is an unlikely explanation for the reduced coherence. The significant IHR–respiration coherence reflects respiratory sinus arrhythmia (RSA), which is modulation of the heart frequency by the amplitude of respiration (113; 98). Wavelet based methods have previously been applied to investigate RSA (46; 36), and Iatsenko et al. (36) found the peak coherence in the respiratory band to decrease with age, suggesting that RSA is more time-variable and weaker in elderly subjects.

Consistent with the previous studies the present results show that the two central pumps of the cardiovascular system, heart and lungs, and their coordination, mainly through RSA, are affected by aging.

4.2. Propagation of the central oscillations: instantaneous heart/respiration rates and oxygenation

Next we investigated the effect of aging on the propagation of cardiovascular oscillations to the brain. Systemic cardiovascular oscillations naturally impact brain oxygenation (44), and their propagation may be affected by age-related structural changes in blood vessels. We investigated this latter possibility by evaluating the phase coherence between the cerebral blood oxygenation and the time-series of instantaneous heart or respiration rates.

The IHR–oxygenation coherence is significantly reduced in the older group in the myogenic and the respiratory frequency bands, across all non-temporal sites (Fig. 5A). These changes in coherence are consistent across combinations, indicating that the changes are systemic. The elastic properties of the vessels are known to change with aging (20), which could affect the propagation of pressure waves and therefore impact the myogenic response, causing reduced IHR–oxygenation coherence. This reduced coherence is attributable to the way in which smooth muscle cells respond to pressure changes. In mice, the myogenic

response to pulsatile pressure in the middle cerebral arteries has been shown to decrease with age (94).

Systemic cardiovascular oscillations have been shown to affect the ~ 0.1 Hz oscillations in cerebral oxygenation: Katura et al. (44) estimated that such effects could only account for less than half of the observed changes. Note, however, that the study investigated heart rate and arterial blood pressure, but did not consider respiration. Furthermore, it has been shown that the Granger causality from heart rate to oxyHb during head-up tilt (93) at 45° decreased with age, which is in line with our findings of reduced coherence in the older group.

In the myogenic frequency band the phase difference between the oscillations in the time-series of IHR and fNIRS is positive, implying that in this frequency interval the oscillations in the IHR are preceding the oscillations recorded by the fNIRS signal. This furthermore confirms that the myogenic oscillations are propagating to the brain. The shift is significantly reduced with ageing, suggesting that the pulse propagates with less resistance to the small vasculature of the brain, as discussed in more detail below in Sec. 4.3.

The phase difference between the same signals in the respiratory band is negative (see Fig. 5A), suggesting that oxygenation is the leading signal. The reduction in phase coherence might, therefore, reflect decreasing efficacy of brain oxygenation with age. However, the phase difference between the two signals in the respiratory band is not altered by ageing.

There is a tendency for the respiration–oxygenation coherence to decrease with age in the respiratory band (at location N5 ~ 0.3 Hz $p < 0.1$, in several locations $p < 0.05$): see Fig. 5B and Fig. 6 in the SM). The phase difference is negative and similar for both groups, suggesting that oxygenation is the leading signal. The high coherence between respiration and each of the oxygenation signals implies a systemic orchestration of cortical oxygenation in rhythm with breathing, an effect that is reduced in the older group. The phase difference, indicating which signal leads or lags the other, can be explained as follows:

688 1. *The oxygenation signal is leading.* Respiration is
689 controlled by the brain stem, and voluntary respira-
690 tion can also be controlled by the motor cortex. The
691 brain then controls the respiration signal.

692
693 2. *The respiration signal is leading.* The period of an
694 oscillation at 0.2 Hz is 5 s, and the period of an oscil-
695 lation at 0.3 Hz is 3.3 s. This means that if the lag is
696 longer than these times the phase difference might ap-
697 pear to be negative when, in reality, it is not. Zhang
698 et al. (115) found in mice that breathing rate is a
699 key modulator of cerebral oxygenation, and that oxy-
700 genation was correlated with both the respiration rate
701 and the phase of the respiration cycle, which was true
702 across the brain. They found a time lag of around
703 1-3 seconds between respiration and PtO₂ consistent
704 with the transit time of blood from the lungs to the
705 brain, which was similar for blood oxygenation too.
706 What a similar lag would be in humans is not known,
707 and the corresponding phase difference is therefore
708 also not known. However, it might be the case that,
709 although the respiration is actually leading the oxy-
710 genation, the latter is delayed by more than the time
711 for one complete respiration cycle.

712 4.3. *Brain oxygenation oscillations and their spatial co-* 713 *herence*

714 The reduced myogenic power and reduced myogenic
715 coherence between the frontal probes, between the
716 frontal-parietal probes and between the occipital probes
717 seen in the older participants (see Fig. 6A,B,C) indicate
718 altered vascular resting state networks.

719
720 There is increased coherence in the cardiac band in the
721 older group, in 50/55 fNIRS combinations (see Fig. 6C),
722 and between fNIRS and EEG signals (see Fig. 7C). This
723 could be explained by several factors, such as the increased
724 radii of vessels in the microvasculature of older participants
725 (16) and decreased microvascular density in older partici-
726 pants (20). While the total cerebral blood flow decreases
727 with age, the pulsatile flow increases (112). It propagates
728 through vessels that are fewer and larger, with reduced
729 surface area per unit volume, resulting in less oxygena-
730 tion. The older group also has decreased vessel elasticity
731 (20) and increased blood pressure (Table 1), and we note
732 that if the cardiac pulse is stronger throughout the smaller
733 vessels, this can cause increased cardiac coherence. These
734 findings are consistent with earlier fNIRS studies as re-
735 ported in the review by Yeung and Chan (114).

736 These results illustrate that, in the brain vasculature,
737 both the oscillations, and their coordination are altered
738 in the older group, suggesting decreased oxygenation of
739 the brain with aging. The myogenic vascular resting state
740 network is weaker in the older group. **We note that our**
741 **definition of resting state networks is mainly operational in**
742 **nature, as participants were recorded while not performing**

any task. However, it is interesting to note that, in addi-
tion to low coherence for the lateral sensors, we observe
strong frontal-parietal coherence. This is consistent with
earlier work (e.g. (84)), and shows that our results also
relate to the placement of the sensors.

4.4. *Neurovascular coherence*

Our key findings are: that there is significant neurovas-
cular phase coherence in the 0.052–0.145 Hz (myogenic)
frequency range; that this coherence is greatly reduced in
older participants, as compared to the younger group; and
that there is higher neurovascular coherence in the cardiac
band in the older group (Fig. 7). As can be seen by com-
paring Figs. 6B,C and 7B, the coherence is also reduced
in some locations without a decrease in power, so that the
reduction in coherence cannot be accounted for by reduced
power. To our knowledge, this is the first report of such
effects.

In both the myogenic and cardiac bands there was
widely distributed coherence across the cortex, as seen in
Fig. 7B,C. In comparison, the neurogenic and respiratory
bands showed little or no significant coherence in either age
group, so that little change in coherence with age could be
detected (see SM Fig. 23). The altered neurovascular co-
herence in the older group reflects less effective neurovascu-
lar interaction. Magnitude squared coherence (which has
linear frequency resolution) between fNIRS and EEG sig-
nals near 0.1 Hz was found in a previous study of healthy
participants aged around 30 years (70). This is in agree-
ment with the coherence found in the younger group of the
present study.

Grooms et al. (29) studied slow oscillations in EEG and
blood oxygen level dependent (BOLD) signals in the de-
fault mode network. The authors concluded that there was
evidence of a relationship between infra-slow (< 0.1 Hz)
EEG and BOLD oscillations at the same frequencies,
which was also found by Hiltunen et al. (32) and Keinänen
et al. (45). These correlations were shown to span sev-
eral brain regions and to be time-varying. Both fNIRS
and BOLD signals reflect changes in oxygenation, and the
BOLD signal has been shown to correlate with both oxyHb
and deoxyHb (100; 90). These studies investigated lin-
ear correlation between BOLD signals and infraslow EEG
time-series, whereas the wavelet phase coherence used in
our present study has logarithmic frequency resolution and
evaluates coherence at each frequency step. The earlier
studies did not consider frequencies above 0.1 Hz, while
our present results show coherence centred around ap-
proximately 0.1 Hz. Although the studies are not directly
comparable, they all provide evidence of a significant rela-
tionship between electrical neural activity and oxygenation
oscillations in the brain at low frequencies. Mitra et al
(64) found a similar relationship in mice, using laminar
electrophysiology and hemoglobin imaging. **Such invasive**
recordings have the advantage of measuring activity that
is more local but, given that our goal was *in-vivo*, non-

798 **invasive measurements in humans, we chose to use EEG**
799 **and fNIRS.**

800 In fMRI studies it is found that typically, only 10% of
801 the variability in the hemodynamic signal can be explained
802 by neural activity (21). Similarly, we show low, but sig-
803 nificant, coherence between the EEG and fNIRS signals.
804 BOLD signals are often thought of as a convolution of the
805 neural activity with what is known as the hemodynamic
806 response function (HRF) (79). The HRF contains vascular
807 factors, such as vasomotion, which is also present in the
808 fNIRS signals. The difference in coherence between the
809 younger and older groups illustrates that care should be
810 taken in studies estimating the HRF, as the response is
811 age-dependent.

812 4.5. Neurovascular coupling

813 In the awake resting state the brain consumes around
814 11% of the cardiac output and 20% of the body’s total
815 metabolic energy, despite only making up about 2% of the
816 body’s weight (30). Resting state functional networks are
817 consistently observed both with fMRI (8; 32) and fNIRS
818 (87), in addition to EEG (4), indicating that the rest-
819 ing state activity is not random. Neurovascular coupling,
820 mediating the adjustment of local cerebral blood flow to
821 match the energy demand of neurons, is maintained con-
822 tinuously by the diverse cells constituting the NVU (35).

823 Studies of neurovascular coupling usually consider in-
824 formation flow from neurons to the vasculature. However,
825 Kim et al. (48) introduced the term vasculo-neuronal cou-
826 pling to describe information flow from vessel to astrocyte
827 to neuron. From experiments on mice, both *in vivo* and *in*
828 *vitro*, the authors concluded that neurons adjust their rest-
829 ing state activity based on brain perfusion changes in flow
830 and pressure (47; 48), probably to match the energy sup-
831 ply and demand. Changes in the blood flow and perfusion
832 are characterised by oscillatory processes, and so is en-
833 ergy metabolism (41). Hence, the energy exchange to the
834 brain is also likely to occur in an oscillatory manner. To
835 be efficient, this is coordinated between the cardiovascular
836 system and the brain, leading to coherent oscillations. It
837 therefore seems likely that the degree of myogenic phase
838 coherence is a proxy for neurovascular efficiency, and that
839 the neurovascular interaction can be considered as arising
840 through the cardiovascular system and brain behaving as
841 interacting oscillators.

842 Myogenic coherence is reduced in the older group of par-
843 ticipants, indicating that the interaction between the os-
844 cillators has decreased. From the current results we can-
845 not be certain of the direction of the interaction, but it
846 could be bi-directional. The neurovascular coherence in
847 the myogenic frequency band is negatively correlated with
848 BMI (Fig. 9), an observation that could be further inves-
849 tigated in future studies.

850 **In the present work we focused on quantifying the func-**
851 **tioning of the neurovascular unit. Our reasoning is that**
852 **the efficiency of coordination between neuronal and vas-**
853 **cular activities can be evaluated by their phase coherence.**

854 It provides a measure of neurovascular coupling. Estab-
855 lishment of the directionality and strength of the coupling
856 between the vascular and neuronal oscillatory modes, as
857 identified in this work, will be the next step in the inves-
858 tigation. The efficiency of the neurovascular unit, and the
859 neurovascular coupling, are of particular interest in rela-
860 tion to the older population, as decreased neurovascular
861 coupling has been linked to cognitive decline and dement-
862 tia (103; 17). Especially promising is the recent report of
863 a treatment that can improve neurovascular coupling in
864 mice (102). Evaluation of neurovascular phase coherence
865 therefore has potential as a biomarker for the efficiency
866 of the NVU, and could be used to evaluate the effects of
867 treatment and lifestyle changes in humans.

868 4.6. Origins of 0.1 Hz oscillations

869 Having established that oxygenation and neural activity
870 are coherent around 0.1 Hz, reflecting neurovascular inter-
871 actions, the next question is: what are the mechanisms
872 underlying the coherence? There are several possible ori-
873 gins of 0.1 Hz oscillations in the brain and cardiovascular
874 system, which we now consider.

875 *Systemic cardiovascular fluctuations.* IHR is coherent
876 with oxygenation at ~ 0.1 Hz (see Sec. 3.2), and, to a much
877 lesser degree respiration is also coherent with oxygenation
878 at ~ 0.1 Hz. However, the systemic cardiovascular fluctua-
879 tions cannot fully explain the oscillations in oxygenation
880 (44), indicating that the 0.1 Hz oscillations could have ad-
881 ditional origins. Most EEG probes have low but non-zero
882 coherence with the ~ 0.1 Hz IHR signal, but the IHR–EEG
883 coherence is generally lower than the neurovascular coher-
884 ence evaluated from the EEG and fNIRS time-series: see
885 SM Fig. 5 and SM Sec. 10.

886 *Vascular origin.* In 1902 Bayliss (6) considered how
887 smooth muscle cells respond to changes in intravascular
888 pressure. This myogenic hypothesis was later studied by
889 Folkow (25) who found it was important for blood autoreg-
890 ulation. Myogenic oscillations tend to manifest between
891 0.052–0.145 Hz (60; 97; 101; 53). Local 0.1 Hz oscillations
892 consistent with myogenic activity have been observed in
893 vivo in the human cortex (81; 72). These oscillations are
894 believed to contribute to the clearance of substances like
895 amyloid-beta proteins from the brain (3).

896 *Vascular neural origin.* The hemodynamic bases of
897 Meyer waves are oscillations of the sympathetic vasomo-
898 tor tone of arterial blood vessels (42). Note that this
899 would contribute to systemic cardiovascular fluctuations
900 by impacting the heart rate and arterial blood pressure.
901 In studies on blood flow with neural blockers, however, it
902 was shown that 0.1 Hz activity continues, suggesting at
903 least a contribution from the myogenic activity (43; 101).
904 Rayshubskiy et al. (81) found that 0.1 Hz oscillations in the
905 human cortex were spatially localised, and correlated with
906 the diameter of local vessels, suggesting that the 0.1 Hz
907 hemodynamic oscillation in the human cortex are primar-
908 ily myogenic in nature.

909 *Electrophysiological origin in the brain.* Oscillations
910 around or below 0.1 Hz detected with EEG in the brain
911 are not traditionally referred to as myogenic, but rather as
912 infra-slow (<0.1 Hz) or slow oscillations (11). Such studies
913 usually do not include measurements of cardiovascular activ-
914 ity, and rather focus on metabolic processes. The origin
915 of these oscillations is still debated (71; 108; 70; 111; 49).
916 Mitra et al (64) have shown that, in mice, the infra-slow os-
917 cillations have unique dynamics when compared to higher
918 frequencies, and should be considered as a separate physi-
919 ological process. There is evidence for both a neuronal and
920 a non-neuronal generator of these oscillations, and possi-
921 bly both of them contribute.

922 One feature of the infra-slow oscillations is that their
923 phases were found to be correlated with the amplitude
924 of faster oscillations and with performance (67; 19). It
925 has been suggested that infra-slow oscillations are related
926 to gross cortical excitability (73) and to arousal (80; 92).
927 Changes in arousal level would be reflected in the heart
928 rate, which could explain why we observe IHR-EEG coher-
929 ence. Non-neuronal infra-slow oscillations in EEG could
930 stem from a potential difference across the blood-brain
931 barrier (BBB) (71; 108; 82; 104; 106). This difference is
932 sensitive to pH (104), and can be manipulated by hypoventi-
933 lation, hyperventilation (108) or postural changes that
934 affect intracranial hemodynamics (106). The BBB, consist-
935 ing of endothelial cells, is known to be affected by aging
936 (91). Further, electrical coupling through the endothelium
937 is a mechanism for neurons to modulate smooth muscle
938 cell activity and therefore arteriole diameter (21). At the
939 molecular level, another component that could affect the
940 slow EEG oscillations might be neural mitochondrial cal-
941 cium signalling, which is known to be altered in aging (86).
942 Neuron-glia interactions are also thought to contribute to
943 the slow oscillations (55; 10), as are extracellular ion fluxes
944 which have been shown to contribute to the coupling of
945 brain activity and blood flow (59).

946 *Other origins.* Another potential origin of infra-slow
947 fluctuations is movement artifacts from fidgeting, which
948 has been observed in both animal and human studies. It
949 has been shown in mice that both flow in arterioles and
950 also brain electrical activity can be impacted by these arti-
951 facts (21), however in humans it is hardly likely that such
952 movement artefacts would be oscillatory.

953 We find widely-distributed ~ 0.1 Hz coherence across
954 the cortex, which does not in itself represent evidence of
955 a single generator. Neurovascular coherence in the myo-
956 genic band is correlated with the IHR-respiration coher-
957 ence in the myogenic band, while the neurovascular coher-
958 ence in the respiratory band is not correlated with the
959 IHR-respiration coherence in the respiratory band. This
960 result suggests that the myogenic frequency band and the
961 0.1 Hz oscillation are key to understanding aging from both
962 the neural and vascular perspectives.

963 4.7. Frequency and amplitude modulation of the γ -band by 964 low-frequency oscillations

965 An interesting question to explore is whether the ampli-
966 tude and/or frequency of γ oscillations in the EEG
967 is modulated by the slower oxygenation/vascular oscilla-
968 tions. Murta et al. (68) have reported evidence for ampli-
969 tude modulation from combined fMRI and EEG studies.
970 There is also some evidence from previous fNIRS studies
971 that β oscillations are modulated by brain oxygenation
972 (77). The ~ 0.1 Hz variations in the oxygenation level of
973 brain blood are generally used as an fMRI-based surrogate
974 of “resting-state” neuronal activity, implying that it is the
975 gamma band which is most closely correlated with BOLD
976 signals (21).

977 To investigate possible amplitude and frequency modu-
978 lation of neuronal activity by low-frequency oxygenation
979 oscillations, we focused on the higher β / lower γ band (20–
980 30 Hz). Our results revealed that the spatial coherence
981 between EEG signals has a peak in this frequency range.
982 They also showed non-zero power for γ -instantaneous fre-
983 quency and γ -instantaneous power time-series between
984 0.007 and 4 Hz, as shown in Figs. 8A, B).

985 We therefore calculated the WPC of the γ -
986 instantaneous frequency time-series with fNIRS (fre-
987 quency modulation), and of the γ -instantaneous power
988 time-series with fNIRS (amplitude modulation) for the
989 8 locations where the fNIRS and EEG are co-located.
990 However, we found little to no coherence in the frequency
991 band considered here (Fig. 8C) indicating that there
992 was no significant frequency modulation. We comment
993 however, that a single γ instantaneous frequency provides
994 only a rough measure of the collective neuronal activity
995 in the γ band.

996 On the other hand, a non-zero coherence was observed
997 for amplitude modulation, as shown in Fig. 8D), though
998 not for all participants. What is more interesting is that we
999 observed a negative phase shift for the older group around
1000 0.06–0.08 Hz. This frequency range is often linked to peri-
1001 odic breathing, which appears in hypoxia (51). This may
1002 indicate that some effects of hypoxia appear with aging,
1003 even in the resting state. These results suggest an exciting
1004 direction for future research through more detailed inves-
1005 tigation of how fast neural activity measured by EEG is
1006 modulated by slow hemodynamic oscillations measured by
1007 fNIRS. Further investigation of the coherence between the
1008 band power and oxygenation should also include a broader
1009 γ frequency band, and could explore other frequency bands
1010 too. This may elucidate additional information about neu-
1011 rovascular interactions.

1012 In addition, neuro-respiratory interactions with the γ -
1013 band may be investigated using the IRR and respira-
1014 tion signals. **Our results show that both the instanta-**
1015 **neous γ -frequency and instantaneous γ -power are modu-**
1016 **lated by respiration (Figure 8A and B).** Earlier studies in
1017 both humans and animals (12; 105; 26) have provided evi-
1018 dence of respiration-related oscillations in several brain re-
1019 gions. Distinct from respiration-related artefacts in fMRI,
1019

1020 respiration-related networks have been shown to be linked
1021 with the γ -band power (105). Respiration-related oscillations
1022 might aid coordination between different brain regions (26). In humans,
1023 the phase of respiration has an impact on memory encoding and perception,
1024 further indicating the importance of respiration for cognitive function.
1025 The close relationship of neural activity to both hemodynamics and
1026 respiration illustrates the importance of simultaneous measurements to
1027 investigate interactions between the underlying systems, e.g. as done in
1028 systemic physiology augmented fNIRS (89).
1029
1030

1031 4.8. Effect of increased BMI and BP

1032 The two age groups differ in BMI and sBP (Table 3).
1033 From Fig. 9A it is clear that BMI is correlated with neurovascular
1034 coherence in the myogenic band.

1035 To separate these effects, we created a smaller data-set,
1036 matching the BMI and BP values between the younger and older groups.
1037 This modified data-sets consisted of 13 younger and 13 older participants
1038 with comparable BMI ($p = 0.80$,) and sBP ($p = 0.86$). We then compared
1039 the subgroups' power/coherence values. The results and subgroup details
1040 are shown in the SM Sec. 9. We conclude that, while it is difficult to
1041 disentangle the influence of ageing from that of the increased BMI/BP,
1042 there is evidence for an effect of ageing on the parameters considered,
1043 independent of the BMI/BP differences.
1044

1045 It is likely that BMI/BP differences also contribute, but some of the
1046 loss of significance can be attributed to loss of statistical power due to
1047 having smaller groups.

1048 Further investigation of the impact of increased BP and BMI could be
1049 useful given that raised BMI is associated with increased risk of
1050 cardiovascular diseases such as coronary heart disease (54), and increased
1051 mid-life BMI is associated with the development of dementia in later life
1052 (74).
1053
1054

1055 5. Conclusions

1056 We have investigated the function of the neurovascular unit at
1057 macroscopic level, evaluating the coherence between the oscillations in
1058 the cardiovascular system (simultaneously monitored centrally via ECG
1059 and respiration effort, and locally by whole-brain fNIRS) and oscillations
1060 in neuronal activity (monitored locally by EEG), thereby gaining insight
1061 into the mechanisms of ageing in the NVU.
1062

1063 Most notably, the neurovascular coherence near 0.1 Hz is significantly
1064 reduced by ageing. This presumably reflects progressively impaired control
1065 of cerebral blood flow. The changes in cardio-respiratory coherence with
1066 blood oxygenation confirm that age affects significantly brain vascular
1067 function and oxygenation. It seems that this then impacts neuronal
1068 activity.
1069

1070 The methods described here, combined with state-of-the-art time-frequency
1071 analysis focusing on phase dynamics, have yielded new insights into the
1072 neurovascular dy-

1073 namics of the aging brain. In particular, they have provided a
1074 quantitative measure of the neurovascular efficiency and health of the
1075 NVU, information that cannot be obtained in other ways. The approach
1076 could thus be used for non-invasive evaluation of the decline of
1077 neurovascular function in normal aging, as well as for monitoring the
1078 efficacy of treatment or lifestyle changes in a wide range of
1079 neurodegenerative disorders.
1080

1081 Code availability

1082 MODA is a numerical toolbox developed by the Lancaster University
1083 Nonlinear Dynamics group (available at <http://doi.org/10.5281/zenodo.3470856>).

1084 The code for the permutation test was based on: Cardillo G. (2008) Rndttest:
1085 An alternative to Student t-test assessing difference in means. <http://www.mathworks.com/matlabcentral/fileexchange/20928>

1086 In addition, these MATLAB functions were used for plotting: Rob Campbell
1087 (2021), <https://github.com/raacampbell/sigstar>, Bastian Bechtold
1088 (2016), Violin Plots for MATLAB, Github Project, <https://github.com/bastibe/Violinplot-Matlab>.
1089
1090
1091
1092
1093

1094 Data availability

1095 The data analysed are available in Lancaster University's Pure database:
1096 <https://doi.org/10.17635/lancaster/researchdata/427>
1097

1098 Funding

1099 The research reported in this paper was funded by the Engineering and
1100 Physical Sciences Research Council (UK) under Grant No. EP/M006298/1,
1101 the Sir John Fisher Foundation, and the Slovene Research Agency (Program
1102 No. P20232). The development of the toolbox MODA used for analysis
1103 was also supported by the Engineering and Physical Sciences Research
1104 Council (UK) Grant No. EP/100999X1, the EU projects BRACCIA [517133]
1105 and COSMOS [642563] and the Action Medical Research (UK) MASDA
1106 Project [GN1963].
1107
1108

1109 References

- 1110 [1] Agelink, M.W., Malessa, R., Baumann, B., Majewski, T., Akila, F.,
1111 Zeit, T., Ziegler, D., 2001. Standardized tests of heart rate variability:
1112 Normal ranges obtained from 309 healthy humans, and effects of age,
1113 gender, and heart rate. *Clin. Auton. Res.* 11, 99–108. 1114
- 1115 [2] Al Zoubi, O., Ki Wong, C., Kuplicki, R.T., Yeh, H.w., Mayeli, A.,
1116 Refai, H., Paulus, M., Bodurka, J., 2018. Predicting age for brain EEG
1117 signals—a machine learning approach. *Front. Aging Neurosci.* 10, 184. 1118
- 1119 [3] Aldea, R., Weller, R.O., Wilcock, D.M., Carare, R.O., Richardson, G.,
1120 2019. Cerebrovascular smooth muscle cells as the drivers of intramural
1121 periarterial drainage of the brain. *Front. Aging Neurosci.* 11. 1122

- [4] Babiloni, C., Binetti, G., Cassarino, A., Dal Forno, G., Del Percio, C., Ferreri, F., Ferri, R., Frisoni, G., Galderisi, S., Hirata, K., Lanuzza, B., Miniussi, C., Mucci, A., Nobili, F., Rodriguez, G., Luca Romani, G., Rossini, P.M., 2006. Sources of cortical rhythms in adults during physiological aging: A multicentric EEG study. *Hum. Brain Mapp.* 27, 162–172.
- [5] Bandrivskyy, A., Bernjak, A., McClintock, P.V.E., Stefanovska, A., 2004. Wavelet phase coherence analysis: Application to skin temperature and blood flow. *Cardiovasc. Eng.* 4, 89–93.
- [6] Bayliss, W.M., 1902. On the local reactions of the arterial wall to changes of internal pressure. *J. Physiol.* 28, 220–231.
- [7] Billman, G., 2011. Heart rate variability – a historical perspective. *Front. Physiol.* 2.
- [8] Biswal, B., Yetkin, F.Z., Haughton, V.M., Hyde, J.S., 1995. Functional connectivity in the motor cortex of resting human brain using echo-planar MRI. *Magn. Reson. Med.* 34, 537–541.
- [9] Brodbeck, V., Spinelli, L., Lascano, A.M., Wissmeier, M., Vargas, M.I., Vuillemoz, S., Pollo, C., Schaller, K., Michel, C.M., Seck, M., 2011. Electroencephalographic source imaging: a prospective study of 152 operated epileptic patients. *Brain* 134, 2887–2897.
- [10] Buzsáki, G., Anastassiou, C.A., Koch, C., 2012. The origin of extracellular fields and currents — EEG, ECoG, LFP and spikes. *Nat. Rev. Neurosci.* 13, 407–420.
- [11] Buzsáki, G., Draguhn, A., 2004. Neuronal oscillations in cortical networks. *Science* 304, 1926–1929.
- [12] Chang, C., Glover, G.H., 2009. Relationship between respiration, end-tidal CO₂, and BOLD signals in resting-state fMRI. *NeuroImage* 47, 1381–1393.
- [13] Clemson, P., Lancaster, G., Stefanovska, A., 2016. Reconstructing time-dependent dynamics. *Proc. IEEE* 104, 223–241.
- [14] Clemson, P.T., Hoag, J.B., Cooke, W.H., Eckberg, D.L., Stefanovska, A., 2022. Beyond the baroreflex: A new measure of autonomic regulation based on the time-frequency assessment of varifront. *physiol.ability, phase coherence and couplings. Front. Net. Physiol.* 2, 891604.
- [15] Cohen, J., 1988. *Statistical Power Analysis for the Behavioral Sciences* (2nd ed.). Lawrence Erlbaum Associates.
- [16] Cox, S.R., Ritchie, S.J., Tucker-Drob, E.M., Liewald, D.C., Hagenaars, S.P., Davies, G., Wardlaw, J.M., Gale, C.R., Bastin, M.E., Deary, I.J., et al., 2016. Ageing and brain white matter structure in 3,513 UK Biobank participants. *Nat. Commun.* 7, 13629.
- [17] Csipo, T., Mukli, P., Lipecz, A., Tarantini, S., Bahadli, D., Abdulhussein, O., Owens, C., Kiss, T., Balasubramanian, P., Nyúl-Tóth, Á., Hand, R. A., Yabluchanska, V., Sorond, F. A., Csiszar, A., Ungvari, Z., Yabluchanskiy, A., 2019. Assessment of age-related decline of neurovascular coupling responses by functional near-infrared spectroscopy (fNIRS) in humans. *Geroscience* 41, 5, 495–509.
- [18] Custo, A., Van De Ville, D., Wells, W.M., Tomescu, M.I., Brunet, D., Michel, C.M., 2017. Electroencephalographic resting-state networks: source localization of microstates. *Brain Connect.* 7, 671–682.
- [19] De Goede, A.A., Van Putten, M.J.A.M., 2019. Infraslow activity as a potential modulator of corticomotor excitability. *J. Neurophysiol.* 122, 325–335.
- [20] Desjardins, M., Berti, R., Lefebvre, J., Dubeau, S., Lesage, F., 2014. Aging-related differences in cerebral capillary blood flow in anesthetized rats. *Neurobiol. Aging* 35, 1947–1955.
- [21] Drew, P.J., Mateo, C., Turner, K.L., Yu, X., Kleinfeld, D., 2020. Ultra-slow oscillations in fMRI and resting-state connectivity: Neuronal and vascular contributions and technical confounds. *Neuron* 107, 782–804.
- [22] Dustman, R., Shearer, D., Emmerson, R., 1999. Life-span changes in EEG spectral amplitude, amplitude variability and mean frequency. *Clin. Neurophysiol.* 110, 1399–1409.
- [23] Faul, F., Erdfelder, E., Lang, A.G., Buchner, A., 2007. G*power 3: A flexible statistical power analysis program for the social, behavioral, and biomedical sciences. *Behav. Res. Methods* 39, 175–191.
- [24] Fjell, A.M., Walhovd, K.B., 2010. Structural brain changes in aging: courses, causes and cognitive consequences. *Rev. Neurosci.* 21, 187–221.
- [25] Folkow, B., 1949. Intravascular pressure as a factor regulating the tone of the small vessels. *Acta Physiol. Scand.* 17, 289–310.
- [26] Folschweiller, S., Sauer, J.F., 2022. Controlling neuronal assemblies: a fundamental function of respiration-related brain oscillations in neuronal networks. *Pflugers. Arch.* 475, 13–21.
- [27] Geovanini, G.R., Vasques, E.R., De Oliveira Alvim, R., Mill, J.G., Andreão, R.V., Vasques, B.K., Pereira, A.C., Krieger, J.E., 2020. Age and sex differences in heart rate variability and vagal specific patterns – Baependi heart study. *Global Heart* 15, 71.
- [28] Gonneaud, J., Baria, A.T., Pichet Binette, A., Gordon, B.A., Chhatwal, J.P., Cruchaga, C., Jucker, M., Levin, J., Salloway, S., Farlow, M., et al., 2021. Accelerated functional brain aging in pre-clinical familial Alzheimer’s disease. *Nat. Commun.* 12, 5346.
- [29] Grooms, J.K., Thompson, G.J., Pan, W.J., Billings, J., Schumacher, E.H., Epstein, C.M., Keilholz, S.D., 2017. Infraslow electroencephalographic and dynamic resting state network activity. *Brain Connect.* 7, 265–280.
- [30] Gusnard, D.A., Raichle, M.E., Raichle, M.E., 2001. Searching for a baseline: functional imaging and the resting human brain. *Nat. Rev. Neurosci.* 2, 685–694.
- [31] Hashemi, A., Pino, L.J., Moffat, G., Mathewson, K.J., Aimone, C., Bennett, P.J., Schmidt, L.A., Sekuler, A.B., 2016. Characterizing population EEG dynamics throughout adulthood. *eNeuro.* 3, 0275–16.2016.
- [32] Hiltunen, T., Kantola, J., Abou Elseoud, A., Lepola, P., Suominen, K., Starck, T., Nikkinen, J., Remes, J., Tervonen, O., Palva, S., Kiviniemi, V., Palva, J.M., 2014. Infra-slow EEG fluctuations are correlated with resting-state network dynamics in fMRI. *J. Neurosci.* 34, 356–362.
- [33] Hintze, J.L., Nelson, R.D., 1998. Violin plots: A box plot-density trace synergism. *Am. Stat.* 52, 181–184.
- [34] Hoshi, H., Shigihara, Y., 2020. Age- and gender-specific characteristics of the resting-state brain activity: a magnetoencephalography study. *Aging* 12, 21613–21637.
- [35] Iadecola, C., 2017. The neurovascular unit coming of age: A journey through neurovascular coupling in health and disease. *Neuron* 96, 17–42.
- [36] Iatsenko, D., Bernjak, A., Stankovski, T., Shiogai, Y., Owen-Lynch, P.J., Clarkon, P.B.M., McClintock, P.V.E., Stefanovska, A., 2013. Evolution of cardiorespiratory interactions with age. *Phil. Trans. R. Soc.* 371, 20110622.
- [37] Iatsenko, D., McClintock, P.V.E., Stefanovska, A., 2015a. Linear and synchrosqueezed time–frequency representations revisited: Overview, standards of use, resolution, reconstruction, concentration, and algorithms. *Digit. Signal Process.* 42, 1–26.
- [38] Iatsenko, D., McClintock, P.V.E., Stefanovska, A., 2015b. Nonlinear mode decomposition: A noise-robust, adaptive decomposition method. *Phys. Rev. E* 92, 032916.
- [39] Iatsenko, D., McClintock, P.V.E., Stefanovska, A., 2016. Extraction of instantaneous frequencies from ridges in time–frequency representations of signals. *Signal Process.* 125, 290–303.
- [40] Intaglietta, M., 1990. Vasomotion and flowmotion: Physiological mechanisms and clinical evidence. *Vasc. Med. Rev.* 1, 101–112.
- [41] Iotti, S., Borsari, M., Bendahan, D., 2010. Oscillations in energy metabolism. *Biochim. Biophys. Acta. Bioenerg.* 1797, 1353–1361.
- [42] Julien, C., 2006. The enigma of Mayer waves: Facts and models. *Cardiovasc. Res.* 70, 12–21.
- [43] Kastrup, J., Bülow, J., Lassen, N.A., 1989. Vasomotion in human skin before and after local heating recorded with laser Doppler flowmetry. A method for induction of vasomotion. *Int. J. Microcirc. Clin. Exp.* 8, 205–215.

- [44] Katura, T., Tanaka, N., Obata, A., Sato, H., Maki, A., 2006. Quantitative evaluation of interrelations between spontaneous low-frequency oscillations in cerebral hemodynamics and systemic cardiovascular dynamics. *NeuroImage* 31, 1592–1600.
- [45] Keinänen, T., Rytty, S., Korhonen, V., Huotari, N., Nikkinen, J., Tervonen, O., Palva, J.M., Kiviniemi, V., 2018. Fluctuations of the EEG-fMRI correlation reflect intrinsic strength of functional connectivity in default mode network. *J. Neurosci. Res.* 96, 1689–1698.
- [46] Keissar, K., Davrath, L.R., Akselrod, S., 2009. Coherence analysis between respiration and heart rate variability using continuous wavelet transform. *Phil. Trans. R. Soc.* 367, 1393–1406.
- [47] Kim, K.J., Iddings, J.A., Stern, J.E., Blanco, V.M., Croom, D., Kirov, S.A., Filosa, J.A., 2015. Astrocyte contributions to flow/pressure-evoked parenchymal arteriole vasoconstriction. *J. Neurosci.* 35, 8245–8257.
- [48] Kim, K.J., Ramiro Diaz, J., Iddings, J.A., Filosa, J.A., 2016. Vasculo-neuronal coupling: Retrograde vascular communication to brain neurons. *J. Neurosci.* 36, 12624–12639.
- [49] Kropotov, J.D., 2022. The enigma of infra-slow fluctuations in the human EEG. *Front. Hum. Neurosci.* 16, 928410.
- [50] Kvandal, P., Landsverk, S.A., Bernjak, A., Stefanovska, A., Kvernmo, H.D., Kirkeboen, K.A., 2006. Low frequency oscillations of the laser Doppler perfusion signal in human skin. *Microvasc. Res.* 72, 120–127.
- [51] Lancaster, G., Debevec, T., Millet, G.P., Poussel, M., Willis, S.J., Mramor, M., Goričar, K., Osredkar, D., Dolžan, V., Stefanovska, A., et al., 2020. Relationship between cardiorespiratory phase coherence during hypoxia and genetic polymorphism in humans. *J. Physiol.* 598, 2001–2019.
- [52] Lancaster, G., Iatsenko, D., Pidde, A., Ticcinelli, V., Stefanovska, A., 2018. Surrogate data for hypothesis testing of physical systems. *Phys. Rep.* 748, 1–60.
- [53] Landsverk, S.A., Kvandal, P., Bernjak, A., Stefanovska, A., Kirkeboen, K.A., 2007. The effects of general anesthesia on human skin microcirculation evaluated by wavelet transform. *Anesth. Analg.* 105, 1012–1019.
- [54] Lassale, C., Tzoulaki, I., Moons, K.G.M., Sweeting, M., Boer, J., Johnson, L., Huerta, J.M., Agnoli, C., Freisling, H., Weiderpass, E., Wennberg, P., van der A, D.L., Arriola, L., Benetou, V., Boeing, H., Bonnet, F., Colorado-Yohar, S.M., m, G., Erikssen, A.K., Ferrari, P., Grioni, S., Johansson, M., Kaaks, R., Katsoulis, M., Katzke, V., Key, T.J., Matullo, G., Melander, O., Molina-Portillo, E., Moreno-Iribas, C., Norberg, M., Overvad, K., Panico, S., s, J.R., Saieva, C., Skeie, G., Steffen, A., Stepien, M., nneland, A., Trichopoulou, A., Tumino, R., van der Schouw, Y.T., Verschuren, W.M.M., Langenberg, C., Di Angelantonio, E., Riboli, E., Wareham, N.J., Danesh, J., Butterworth, A.S., 2018. Separate and combined associations of obesity and metabolic health with coronary heart disease: a pan-European case-cohort analysis. *Eur. Heart J.* 39, 397–406.
- [55] Lőrincz, M.L., Geall, F., Ying, B., Crunelli, V., Hughes, S.W., 2009. ATP-dependent infra-slow (< 0.1 Hz) oscillations in thalamic networks. *PLOS ONE* 4, e4447.
- [56] Li, Y., Xie, L., Huang, T., Zhang, Y., Zhou, J., Qi, B., Wang, X., Chen, Z., Li, P., 2019. Aging neurovascular unit and potential role of DNA damage and repair in combating vascular and neurodegenerative disorders. *Front. Neurosci.* 13, 778.
- [57] Li, Z., Zhang, M., Xin, Q., Luo, S., Cui, R., Zhou, W., Lu, L., 2013. Age-related changes in spontaneous oscillations assessed by wavelet transform of cerebral oxygenation and arterial blood pressure signals. *J. Cereb. Blood Flow Metab.* 33, 692–699.
- [58] Maris, E., Oostenveld, R., 2007. Nonparametric statistical testing of EEG- and MEG-data. *J. Neurosci. Methods* 164, 177–190.
- [59] Mathiesen, C., Caesar, K., Akgören, N., Lauritzen, M., 1998. Modification of activity-dependent increases of cerebral blood flow by excitatory synaptic activity and spikes in rat cerebellar cortex. *J. Physiol.* 512, 555–566.
- [60] Mayhew, J.E., Askew, S., Zheng, Y., Porrill, J., Westby, G.W., Redgrave, P., Rector, D.M., Harper, R.M., 1996. Cerebral vasomotion: A 0.1-Hz oscillation in reflected light imaging of neural activity. *NeuroImage* 4, 183–193.
- [61] Meghdadi, A.H., Stevanović Karić, M., McConnell, M., Rupp, G., Richard, C., Hamilton, J., Salat, D., Berka, C., 2021. Resting state EEG biomarkers of cognitive decline associated with Alzheimer’s disease and mild cognitive impairment. *PLOS ONE* 16, 1–31.
- [62] Mesquita, R. C. , Franceschini, M. A. , Boas, D. A. , 2010. Resting state functional connectivity of the whole head with near-infrared spectroscopy. *Biomed. Opt. Express.* 1, 1 324–336.
- [63] Michel, C.M., Brunet, D., 2019. EEG Source Imaging: A Practical Review of the Analysis Steps. *Front. Neurol.* 10, 325.
- [64] Mitra, A., Kraft, A., Wright, P., Acland, B., Snyder, A. Z., Rosenthal, Z., Czerniewski, L., Bauer, A., Snyder, L., Culver, J., Lee, J., Raichle, M. E., 2018. Spontaneous infra-slow brain activity has unique spatiotemporal dynamics and laminar structure. *Neuron* 98, 2, 297-305.e6.
- [65] Moezzi, B., Pratti, L.M., Hordacre, B., Graetz, L., Berryman, C., Lavrencic, L.M., Ridding, M.C., Keage, H.A., McDonnell, M.D., Goldsworthy, M.R., 2019. Characterization of young and old adult brains: An EEG functional connectivity analysis. *Neuroscience* 422, 230–239.
- [66] Montez, T., Poil, S.S., Jones, B.F., Manshanden, I., Verbunt, J.P.A., Van Dijk, B.W., Brussaard, A.B., Van Ooyen, A., Stam, C.J., Scheltens, P., et al., 2009. Altered temporal correlations in parietal alpha and prefrontal theta oscillations in early-stage Alzheimer disease. *Proc. Natl. Acad. Sci. U.S.A.* 106, 1614–1619.
- [67] Monto, S., Palva, S., Voipio, J., Palva, J.M., 2008. Very slow EEG fluctuations predict the dynamics of stimulus detection and oscillation amplitudes in humans. *J. Neurosci.* 28, 8268–8272.
- [68] Murta, T., Leite, M., Carmichael, D.W., Figueiredo, P., Lemieux, L., 2015. Electrophysiological correlates of the BOLD signal for EEG-informed fMRI. *Hum. Brain Mapp.* 36, 391–414.
- [69] Newman, J., Lancaster, G., Stefanovska, A., 2018. Multiscale Oscillatory Dynamics Analysis User Manual v1.01. Department of Physics, Lancaster University.
- [70] Nikulin, V.V., Fedele, T., Mehnert, J., Lipp, A., Noack, C., Steinbrink, J., Curio, G., 2014. Monochromatic ultra-slow (~0.1Hz) oscillations in the human electroencephalogram and their relation to hemodynamics. *NeuroImage* 97, 71–80.
- [71] Nita, D., Vanhatalo, S., Lafortune, F., Voipio, J., Kaila, K., Amzica, F., 2004. Nonneuronal origin of CO₂-related DC EEG shifts: An in vivo study in the cat. *J. Neurophysiol.* 92, 1011–1022.
- [72] Noordmans, H.J., van Blooijis, D., Siero, J.C.W., Zwanenburg, J.J.M., Klaessens, J.H.G.M., Ramsey, N.F., 2018. Detailed view on slow sinusoidal, hemodynamic oscillations on the human brain cortex by Fourier transforming oxy/deoxy hyperspectral images. *Hum. Brain. Mapp.* 39, 3558–3573.
- [73] Palva, J.M., Palva, S., 2012. Infra-slow fluctuations in electrophysiological recordings, blood-oxygenation-level-dependent signals, and psychophysical time series. *NeuroImage* 62, 2201–2211.
- [74] Pedditzi, E., Peters, R., Beckett, N., 2016. The risk of overweight/obesity in mid-life and late life for the development of dementia: a systematic review and meta-analysis of longitudinal studies. *Age Ageing* 45, 14–21.
- [75] Peng, T., Ainslie, P.N., Cotter, J.D., Murrell, C., Thomas, K., Williams, M.J.A., George, K., Shave, R., Rowley, A.B., Payne, S.J., 2008. *Physiol. Meas.* 29, 1055.
- [76] Peters, M.J., Joehanes, R., Pilling, L.C., Schurmann, C., Conneely, K.N., Powell, J., Reinmaa, E., Sutphin, G.L., Zhernakova, A., Schramm, K., et al., 2015. The transcriptional landscape of age in human peripheral blood. *Nat. Commun.* 6, 1–10.

- 6, 8570.
- [77] Pfurtscheller, G., Daly, I., Bauernfeind, G., Müller-Putz, G.R., 2012. Coupling between intrinsic prefrontal HbO2 and central EEG beta power oscillations in the resting brain. *PLOS ONE* 7, e43640.
- [78] Pinto, E., 2007. Blood pressure and ageing. *Postgrad. Med. J.* 83, 109–114.
- [79] Rangaprakash, D., Wu, G.R., Marinazzo, D., Hu, X., Deshpande, G., 2018. Hemodynamic response function (HRF) variability confounds resting-state fMRI functional connectivity. *Magn. Reson. Med.* 80, 1697–1713.
- [80] Raut, R.V., Snyder, A.Z., Mitra, A., Yellin, D., Fujii, N., Malach, R., Raichle, M.E., 2021. Global waves synchronize the brain’s functional systems with fluctuating arousal. *Sci. Adv.* 7.
- [81] Rayshubskiy, A., Wojtasiewicz, T.J., Mikell, C.B., Bouchard, M.B., Timerman, D., Youngerman, B.E., McGovern, R.A., Otten, M.L., Canoll, P., McKhann, G.M., Hillman, E.M., 2014. Direct, intraoperative observation of 0.1 Hz hemodynamic oscillations in awake human cortex: implications for fMRI. *NeuroImage* 87, 323–331.
- [82] Revest, P.A., Jones, H.C., Abbott, N.J., 1993. The transendothelial DC potential of rat blood-brain barrier vessels in situ, in: Drewes, L.R., Betz, A.L. (Eds.), *Frontiers in Cerebral Vascular Biology: Transport and Its Regulation*. Springer US, Boston, MA, pp. 71–74.
- [83] Richard Clark, C., Veltmeyer, M.D., Hamilton, R.J., Simms, E., Paul, R., Hermens, D., Gordon, E., 2004. Spontaneous alpha peak frequency predicts working memory performance across the age span. *Int. J. Psychophysiol.* 53, 1–9.
- [84] Sadaghiani, S., Scheeringa, R., Lehongre, K., Morillon, B., Giraud, A. L., D’Esposito, M., Kleinschmidt, A., 2012. Alpha-band phase synchrony is related to activity in the frontoparietal adaptive control network. *J. Neurosci.* 32, 41, 14305–14310.
- [85] Salerud, E.G., Tenland, T., Nilsson, G.E., Oberg, P.A., 1983. Rhythmical variations in human skin blood flow. *Int. J. Microcirc. Clin. Exp.* 2, 91–102.
- [86] Sanganahalli, B.G., Herman, P., Hyder, F., Kannurpatti, S.S., 2013. Mitochondrial functional state impacts spontaneous neocortical activity and resting state fMRI. *PLOS ONE* 8, e63317.
- [87] Sasai, S., Homae, F., Watanabe, H., Sasaki, A.T., Tanabe, H.C., Sadato, N., Taga, G., 2012. A NIRS-fMRI study of resting state network. *NeuroImage* 63, 179–193.
- [88] Scally, B., Burke, M.R., Bunce, D., Delvenne, J.F., 2018. Resting-state EEG power and connectivity are associated with alpha peak frequency slowing in healthy aging. *Neurobiol. Aging.* 71, 149 – 155.
- [89] Scholkmann, F., Tachtsidis, I., Wolf, M., Wolf, U., 2022. Systemic physiology augmented functional near-infrared spectroscopy: a powerful approach to study the embodied human brain. *Neurophotonics* 9, 030801.
- [90] Schroeter, M.L., Kupka, T., Mildner, T., Uludağ, K., von Cramon, D.Y., 2006. Investigating the post-stimulus undershoot of the BOLD signal – a simultaneous fMRI and fNIRS study. *NeuroImage* 30, 349–358.
- [91] Shioagai, Y., Stefanovska, A., McClintock, P.V.E., 2010. Non-linear dynamics of cardiovascular ageing. *Phys. Rep.* 488, 51–110.
- [92] Sihn, D., Kim, S.P., 2022. Brain Infraslow Activity Correlates With Arousal Levels. *Front. Neurosci.* 16, 765585.
- [93] Song, S., Kim, D., Jang, D.P., Lee, J., Lee, H., Lee, K.M., Kim, I.Y., 2015. Low-frequency oscillations in cerebrovascular and cardiovascular hemodynamics: Their interrelationships and the effect of age. *Microvasc. Res.* 102, 46–53.
- [94] Springo, Z., Toth, P., Tarantini, S., Ashpole, N. M., Tucsek, Z., Sonntag, W. E., Csiszar, A., Koller, A., Ungvari, Z. I., 2015. Aging impairs myogenic adaptation to pulsatile pressure in mouse cerebral arteries. *J. Cereb. Blood Flow Metab.* 35, 4, 527–530.
- [95] Stankovski, T., Pereira, T., McClintock, P. V. E., Stefanovska, A., 2017. Coupling functions: Universal insights into dynamical interaction mechanisms. *Rev. Mod. Phys.*, 89, 045001.
- [96] Stankovski, T., Pereira, T., McClintock, P. V. E., Stefanovska, A., 2019. Introduction. Coupling functions: dynamical interaction mechanisms in the physical, biological and social sciences. *Phil. Trans. R. Soc. Lond. A*, 377, 20190039.
- [97] Stefanovska, A., 2007. Coupled oscillators: Complex but not complicated cardiovascular and brain interactions. *IEEE Eng. Med. Biol. Mag.* 26, 25–29.
- [98] Stefanovska, A., Bračić, M., 1999. Physics of the human cardiovascular system. *Contemp. Phys.* 40, 31–55.
- [99] Stefanovska, A., Hožič, M., 2000. Spatial synchronization in the human cardiovascular system. *Prog. Theor. Phys. Suppl.* 139, 270–282.
- [100] Strangman, G., Culver, J.P., Thompson, J.H., Boas, D.A., 2002. A quantitative comparison of simultaneous BOLD fMRI and NIRS recordings during functional brain activation. *NeuroImage* 17, 719–731.
- [101] Söderström, T., Stefanovska, A., Veber, M., Svensson, H., 2003. Involvement of sympathetic nerve activity in skin blood flow oscillations in humans. *Am. J. Physiol. Heart Circ. Physiol.* 284, H1638–1646.
- [102] Tarantini, S., Yabluchanskiy, A., Csipo, T., Fulop, G., Kiss, T., Balasubramanian, P., Delfavero, J., Ahire, C., Ungvari, A., Nyúl-Tóth, Á., Farkas, E., Benyo, Z., Tóth, A., Csiszar, A., Ungvari, Z., 2019. Treatment with the poly(ADP-ribose) polymerase inhibitor PJ-34 improves cerebrovascular endothelial function, neurovascular coupling responses and cognitive performance in aged mice, supporting the NAD+ depletion hypothesis of neurovascular aging. *GeroScience* 41, 5, 533–542.
- [103] Tarantini, S., Tran, C. H. T., Gordon, G. R., Ungvari, Z., Csiszar, A., 2017. Impaired neurovascular coupling in aging and Alzheimer’s disease: Contribution of astrocyte dysfunction and endothelial impairment to cognitive decline. *Exp. Gerontol.* 94, 52–58.
- [104] Tschirgi, R.D., Taylor, J.L., 1958. Slowly changing bioelectric potentials associated with the blood-brain barrier. *Am. J. Physiol.* 195, 7–22.
- [105] Tu, W., Zhang, N., 2022. Neural underpinning of a respiration-associated resting-state fMRI network. *eLife* 11, e81555.
- [106] Vanhatalo, S., Tallgren, P., Becker, C., Holmes, M.D., Miller, J.W., Kaila, K., Voipio, J., 2003. Scalp-recorded slow EEG responses generated in response to hemodynamic changes in the human brain. *Clin. Neurophysiol.* 114, 1744–1754.
- [107] Veldsman, M., Tai, X.Y., Nichols, T., Smith, S., Peixoto, J., Manohar, S., Husain, M., 2020. Cerebrovascular risk factors impact frontoparietal network integrity and executive function in healthy ageing. *Nat. Commun.* 11, 4340.
- [108] Voipio, J., Tallgren, P., Heinonen, E., Vanhatalo, S., Kaila, K., 2003. Millivolt-scale DC shifts in the human scalp EEG: Evidence for a nonneuronal generator. *J. Neurophysiol.* 89, 2208–2214.
- [109] Vysata, O., Kukal, J., Prochazka, A., Pazdera, L., Simko, J., Valis, M., 2014. Age-related changes in EEG coherence. *Neurol. Neurochir. Pol.* 48, 35–38.
- [110] Wang, B., Zhang, M., Bu, L., Xu, L., Wang, W., Li, Z., 2016. Posture-related changes in brain functional connectivity as assessed by wavelet phase coherence of NIRS signals in elderly subjects. *Behav. Brain Res.* 312, 238–245.
- [111] Watson, B.O., 2018. Cognitive and physiologic impacts of the infraslow oscillation. *Front. Syst. Neurosci.* 12, 44.
- [112] Xu, X., Wang, B., Ren, C., Hu, J., Greenberg, D.A., Chen, T., Xie, L., Jin, K., 2017. Age-related impairment of vascular structure and functions. *Aging Dis.* 8, 590–610.
- [113] Yasuma, F., Hayano, J., 2004. Respiratory sinus arrhythmia: Why does the heartbeat synchronize with respiratory rhythm? *Chest* 125, 683–690.
- [114] Yeung, M.K., Chan, A.S., 2021. A systematic review of the application of functional near-infrared spectroscopy to the study of cerebral hemodynamics in healthy aging. *Neuropsychol.*

1549 Rev. 31, 139–166.
1550 [115] Zhang, Q., Roche, M., Gheres, K.W., Chaigneau, E.,
1551 Kedarasetti, R.T., Haselden, W.D., Charpak, S., Drew, P.J.,
1552 2019. Cerebral oxygenation during locomotion is modulated
1553 by respiration. *Nat. Commun.* 10, 5515.

1554 **Acknowledgements**

1555 We are grateful to all the participants for taking part in
1556 the study. We would like to thank Franci Benko, research
1557 nurse at the Department of Neurology, University Medical
1558 Centre Ljubljana, for his help in organising and carrying
1559 out the measurements, and Fajko Bajrović for his support
1560 with the clinical part of the study. In addition, we would
1561 like to thank Boštjan Dolenc for the automated analysis
1562 used for initial checks, and Cheryl Hawkes and Christo-
1563 pher Gaffney for helpful comments on the manuscript. JB
1564 is grateful to Benediktas Valys, Joe Rowland Adams and
1565 Charlie Mpetha for useful discussions, and to Sam Mc-
1566 Cormack for help with programming. JB is funded by a
1567 PhD scholarship grant awarded to TJC by the Sir John
1568 Fisher Foundation. The High End Computing facility at
1569 Lancaster University was used for data analysis.

1570 **Author contributions**

1571 GL did the measurements and preliminary analysis of
1572 the data. JK and BM organised all clinical aspects of the
1573 study. JB analysed the data completely, prepared the fig-
1574 ures and a draft of the text. PVEMcC contributed to
1575 writing the funding proposal. TJC supervised JB and
1576 advised on writing the manuscript. AS conceived the
1577 study, wrote the funding proposal, provided the theoret-
1578 ical framework for the time-series analysis methods, se-
1579 lected and discussed the analysis methods, supervised GL
1580 and JB and closely discussed the results. She was also
1581 involved in structuring the manuscript. All authors con-
1582 tributed to editing the manuscript, and accepted the final
1583 version.

1584 **Conflict of interest**

1585 The authors have no conflict of interest.